

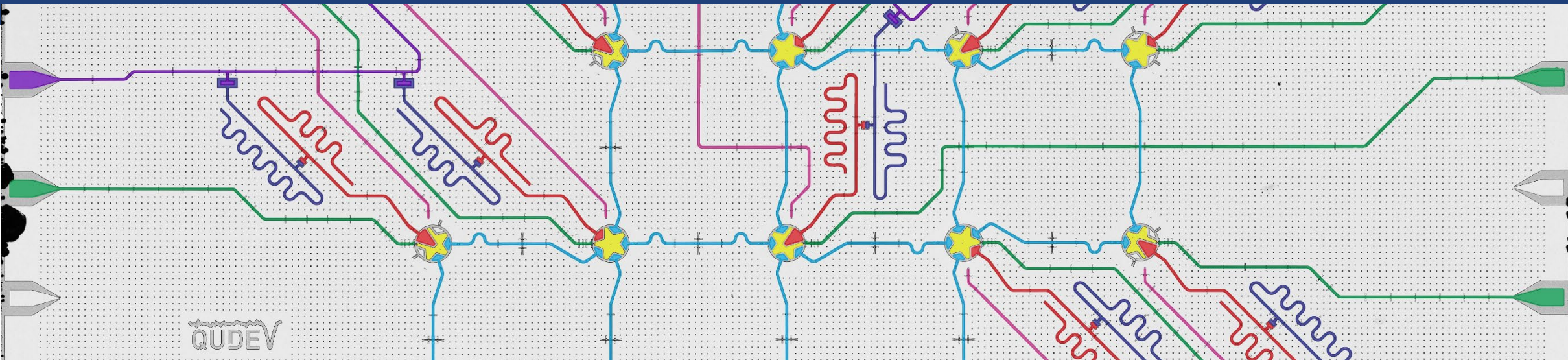
1 mm

QUDEV

SCAN ME



The Slides



Quantum Error Correction with Superconducting Circuits

Sci. Team: E. Al-Tavil, L. Beltran, I. Besedin, J.-C. Besse, D. Colao Zanuz, Xi Dai, K. Dalton, J. Ekert, S. Frasca, A. Grigorev, D. Hagmann, C. Hellings, A. Hernandez-Anton, I. Hesner, L. Hofele, M. Kerschbaum, J. Knoll, A. Kulikov, N. Lacroix, M. Pechal, K. Reuer, A. Rosario, C. Scarato, J. Schaer, Y. Song, F. Swiadek, J. Trebst, F. Wagner, A. Wallraff (ETH Zurich)

L. Bödeker, L. Colmenarez, M. Müller (RWTH Aachen)

Eng. & Tech. Team: M. Bahrani, A. Flasby (ETH Zurich)

Innovation project
supported by



Schweizerischer
Nationalfonds

Schweizerische Eidgenossenschaft
Confédération suisse
Confederazione Svizzera
Confederaziun svizra
Swiss Confederation
Innosuisse – Swiss Innovation Agency

The Quantum Device Lab



Schweizerischer
Nationalfonds

Innovation project
supported by



Schweizerische Eidgenossenschaft
Confédération suisse
Confederazione Svizzera
Confederaziun svizra
Swiss Confederation



Innosuisse – Swiss Innovation Agency



IARPA
BE THE FUTURE

with spring-term project students

Past Group Members & Current Collaboration Partners

www.qudev.ethz.ch

Former group members now Faculty/PostDoc/PhD/Industry

A. Abdumalikov (Gorba AG)
M. Allan (LMU Munich)
C. K. Andersen (TU Delft)
M. Baur (ABB)
J. Basset (U. Paris Sud)
S. Berger (AWK Group)
R. Bianchetti (ABB)
D. Bozyigit (Scandit)
R. D. Buijs (ASML)
M. Collodo (Zurich Instruments)
A. Copetudo (NU Singapore)
C. Eichler (FAU Erlangen)
A. Fedorov (UQ Brisbane)
Q. Ficheux (CNRS Grenoble)
S. Filipp (WMI & TU Munich)
J. Fink (IST Austria)
A. Fragner (Kappa)
T. Frey (Bosch)
M. Gabureac (PSI)
S. Garcia (College de France)
S. Gasparinetti (Chalmers)
M. Goppl (Sensirion)
J. Govenius (VTT)

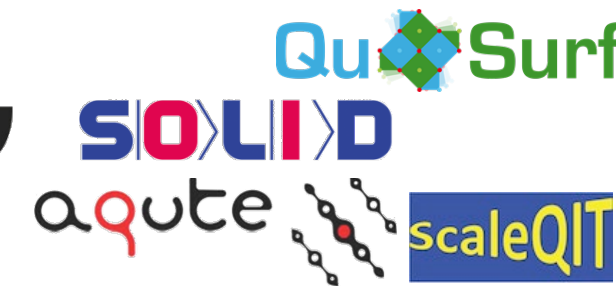
J. Heinsoo (IQM)
J. Herrmann (QuantrolOx)
L. Huthmacher (Stellbrink & Prtnr)
D.-D. Jarausch (Leica)
K. Juliusson (IQM)
P. Kurpiers (Rohde & Schwarz)
J. Krause (U. Of Cologne)
S. Krinner (Zurich Instruments)
N. Lacroix (Google)
C. Lang (Radionor)
S. Lazar (Zurich Instruments)
P. Leek (Oxford)
S. M. Llima (BSC-CNS)
J. Luetolf (D-PHYS, ETH Zurich)
P. Magnard (Alice and Bob)
P. Maurer (Chicago)
J. Mlynek (Siemens)
M. Mondal (IACS Kolkata)
G. Norris (AWS)
M. Oppliger
J. O'Sullivan (CEA Saclay)
A. Potocnik (imec)
G. Puebla (QZabre)
A. Rumm (Atlantic Quantum)
A. Safavi-Naeini (Stanford)

Y. Salathe (Zurich Instruments)
P. Scarlino (EPF Lausanne)
M. Stammeier (Huba Control)
L. Steffen (AWK Group)
A. Stockklauser (Rigetti)
T. Thiele (Zurich Instruments)
I. Tsitsilin (TUM)
J. Ungerer (Harvard)
A. van Loo (RIKEN)
D. van Woerkom (Microsoft)
J. Waissman (HUJI)
T. Walter (deceased)
L. Wernli (Sensirion)
A. Wulff
S. Zeytinoğlu (Harvard)

K. Ensslin (ETH Zurich)
M. Hartmann (FAU Erlangen)
T. Ihn (ETH Zurich)
A. Imamoğlu (ETH Zurich)
F. Marquardt (MPL Erlangen)
F. Merkt (ETH Zurich)
A. Messmer (Zurich Instruments)
M. W. Mitchell (ICFO)
M. Müller (RWTH Aachen, FZJ)
M. A. Martin-Delgado (Madrid)
M. Poggio (Basel)
B. Royer (Sherbrooke)
N. Sangouard (CEA Saclay)
H. Tureci (Princeton)
W. Wegscheider (ETH Zurich)

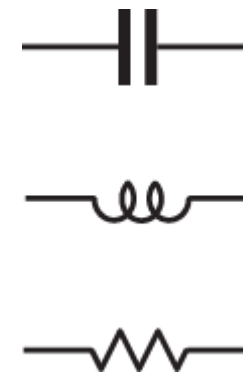
Collaborations (last 5 years) with groups of

C. Abellan (Quside)
P. Bertet (CEA Saclay)
A. Blais (Sherbrooke)
J. Bylander (Chalmers)
H. J. Carmichael (Auckland)
A. Chin (Cambridge)
I. Cirac (MPQ)

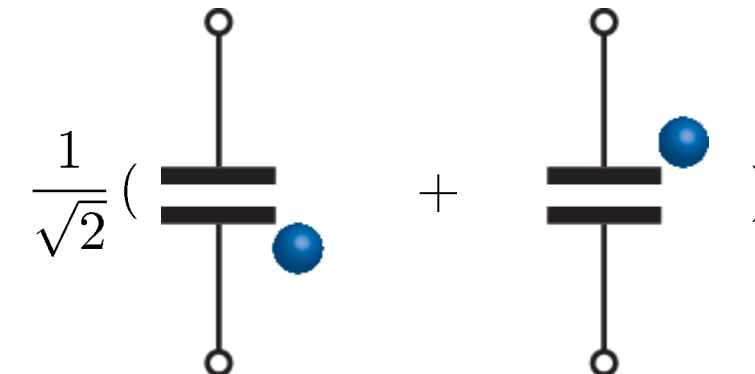


Quantum Physics with Electronic Circuits

basic circuit elements:



charge on a capacitor:



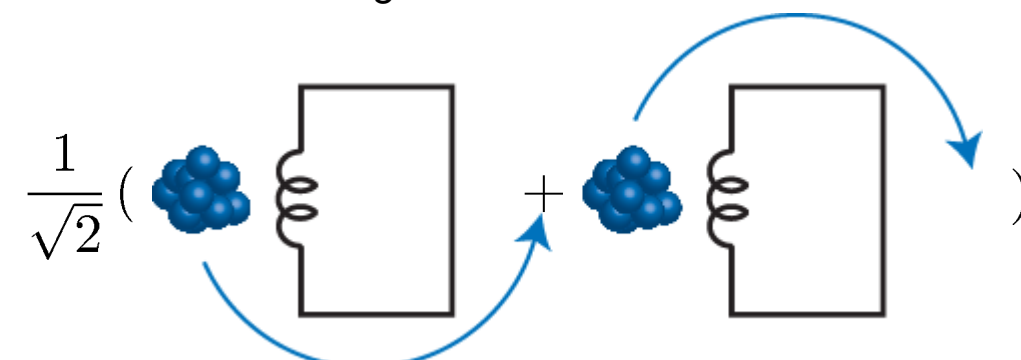
quantum superposition states of:

- charge Q
- flux ϕ

Q, ϕ are conjugate variables

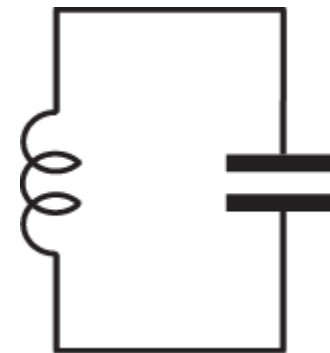
commutation relation $[\hat{\phi}, \hat{Q}] = i\hbar$

current or magnetic flux in an inductor:

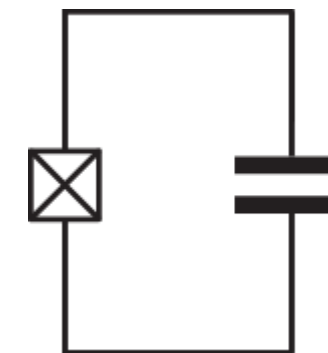


Linear and Nonlinear Superconducting Electronic Oscillators

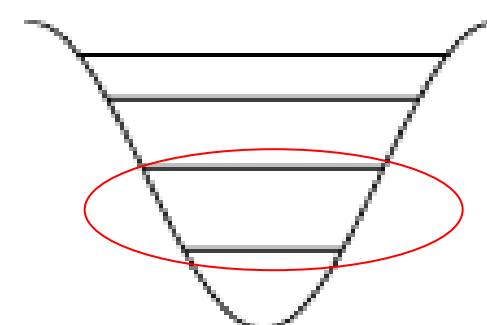
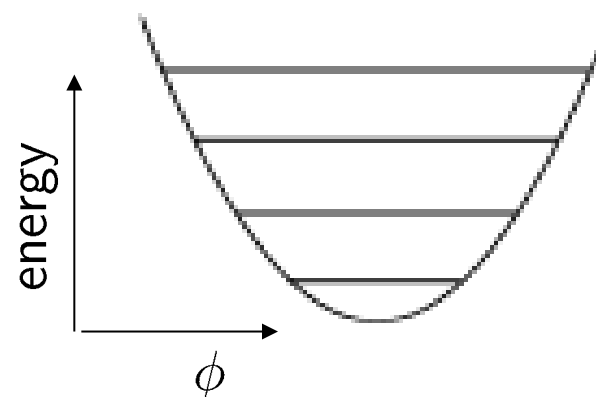
LC resonator:



Josephson junction resonator:
Josephson junction = nonlinear inductor



anharmonicity defines effective two-level system

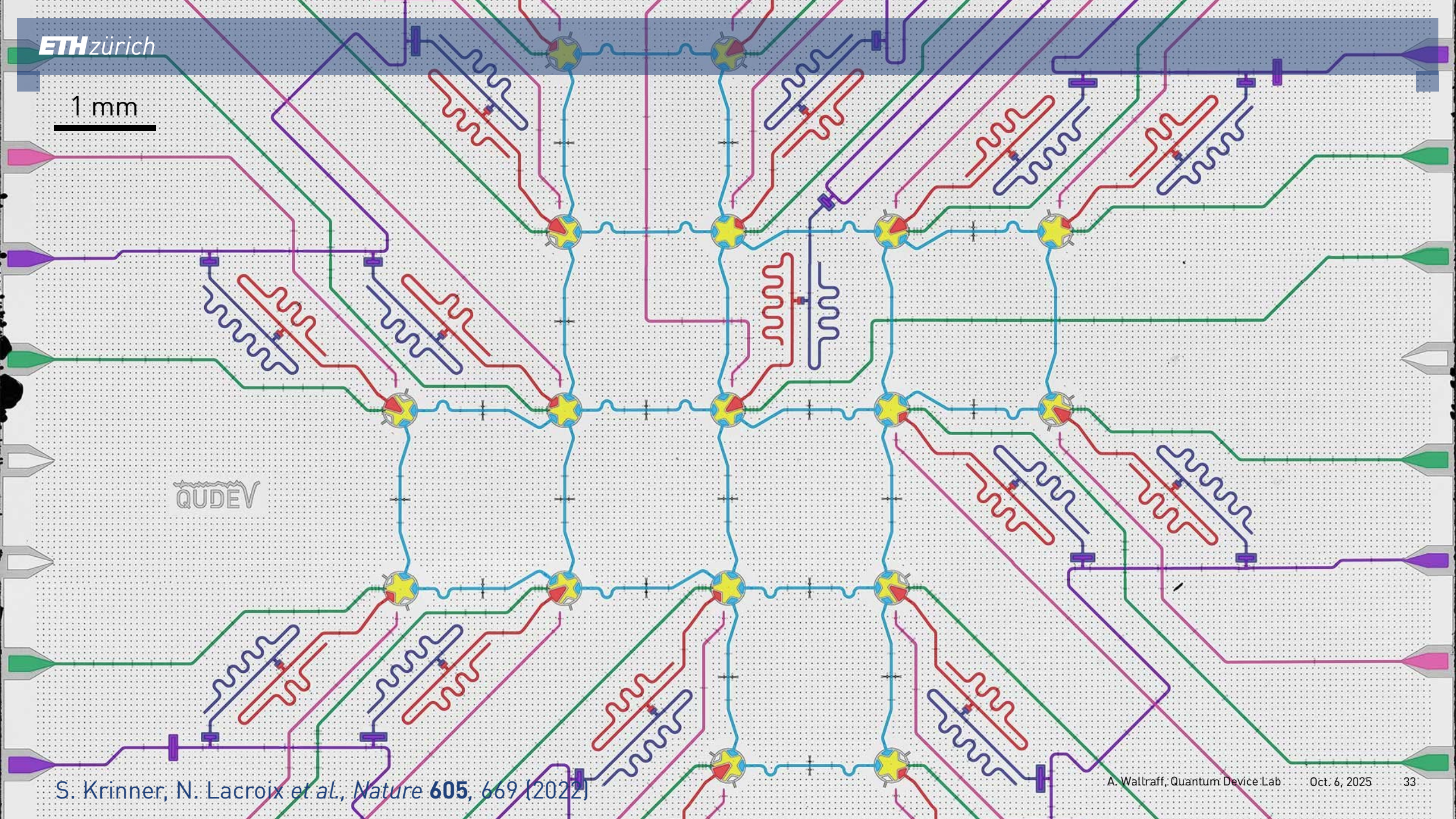


1 mm

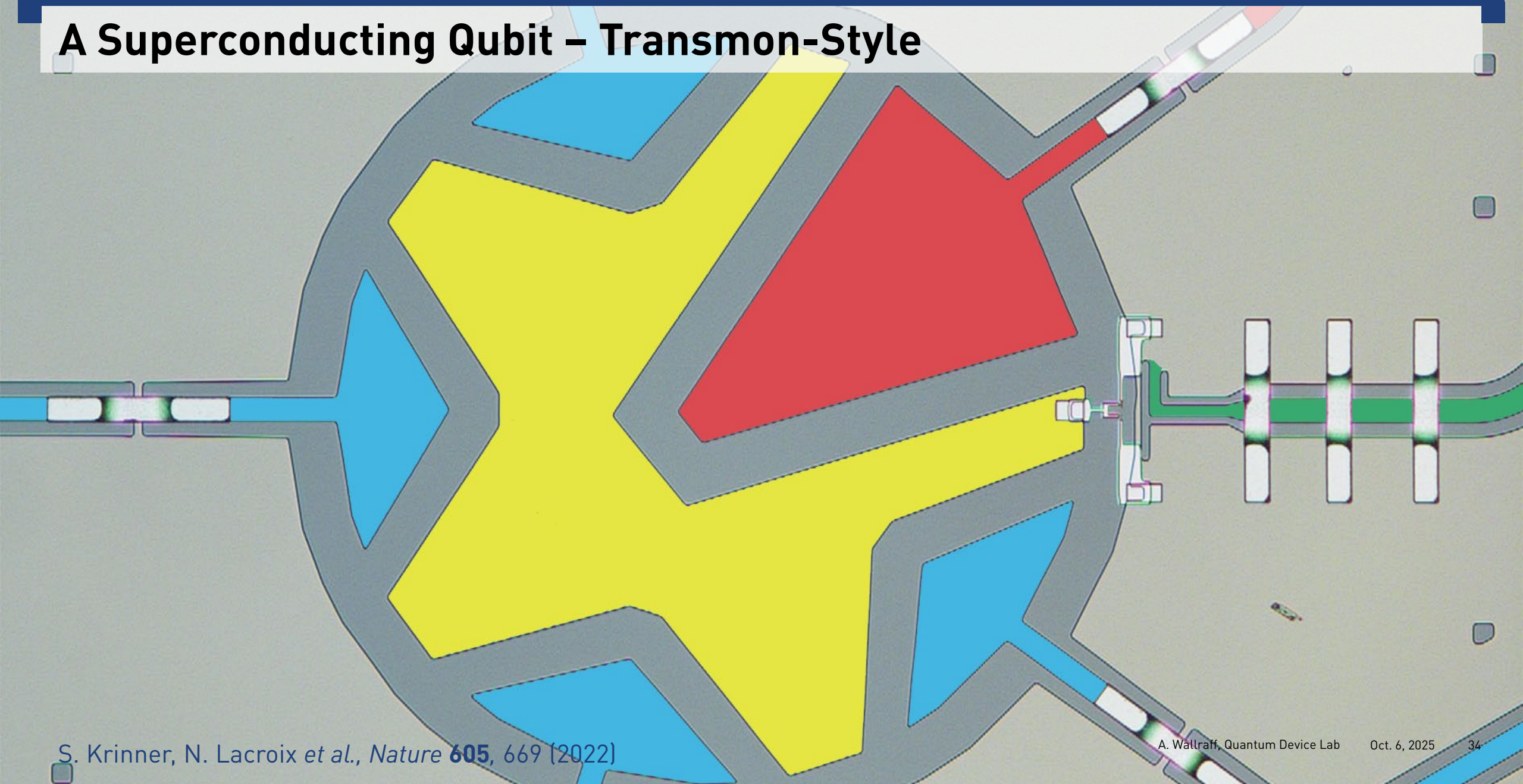
17 Qubits, with 24 Coplanar Waveguide Resonators for Two-Qubit Coupling
and 17 Resonator-Purcell-Filter Pairs for Qubit Readout.

1 mm

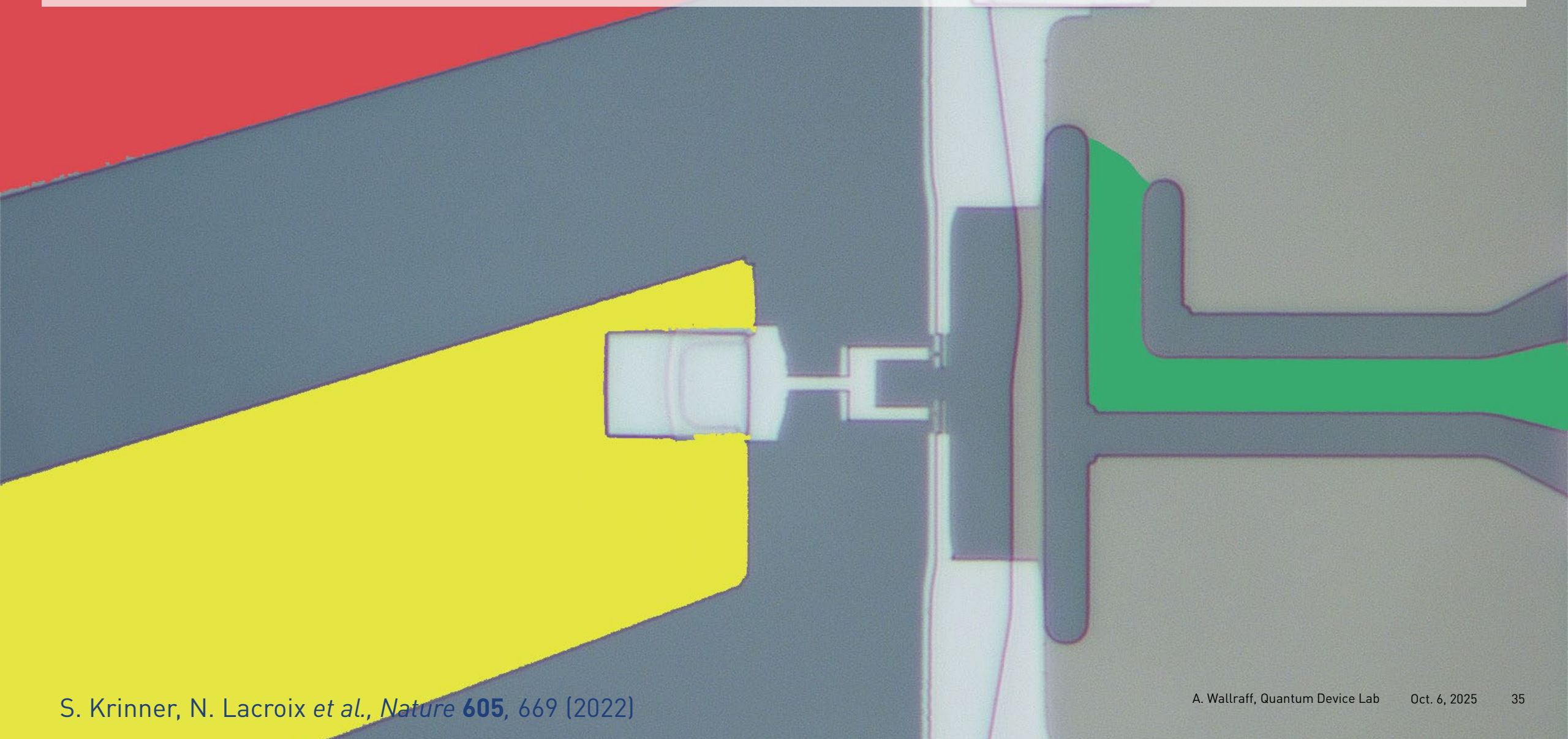
QUDEV



A Superconducting Qubit – Transmon-Style



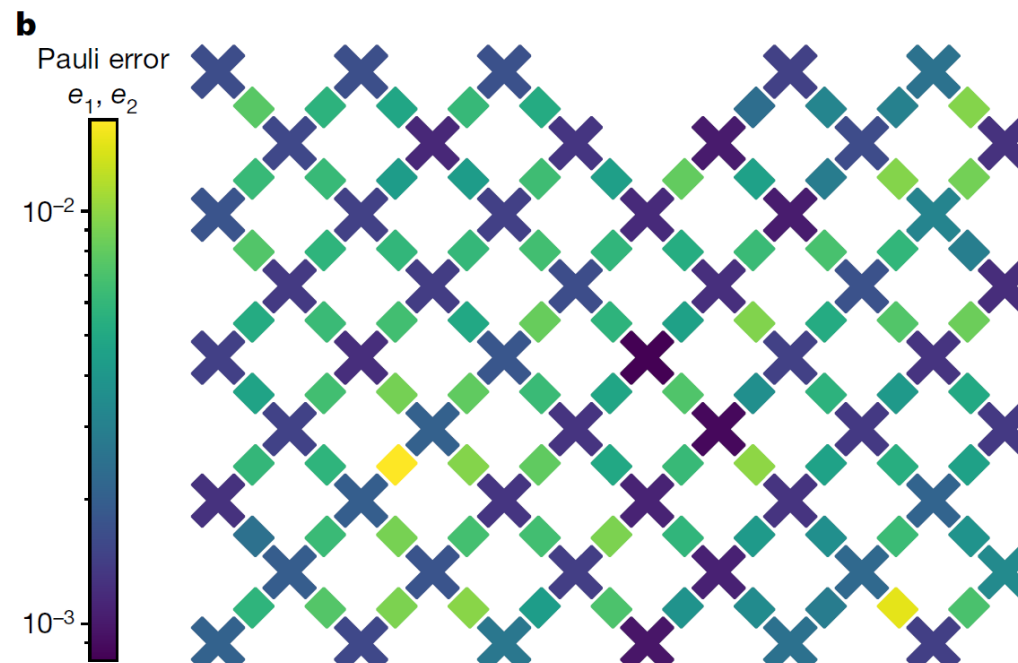
Tunnel Junctions, SQUID, and Fluxline



Two of the Major Goals in Quantum Information Processing ...

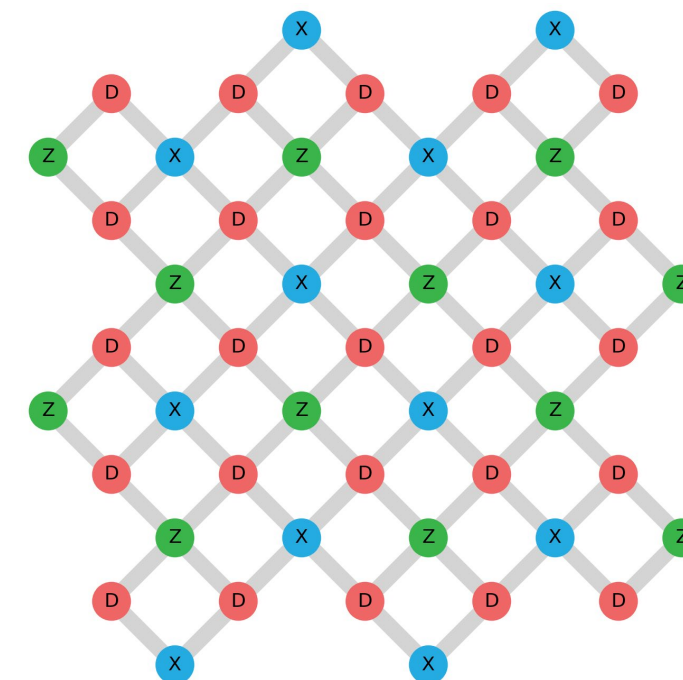
... with superconducting circuits

Noisy Intermediate Scale Quantum (NISQ)
algorithms displaying a quantum advantage



F. Arute, ..., J. M. Martinis *et al.*, *Nature* **574**, 505 (2019)

Fault-tolerant, error-corrected, universal
quantum information processor

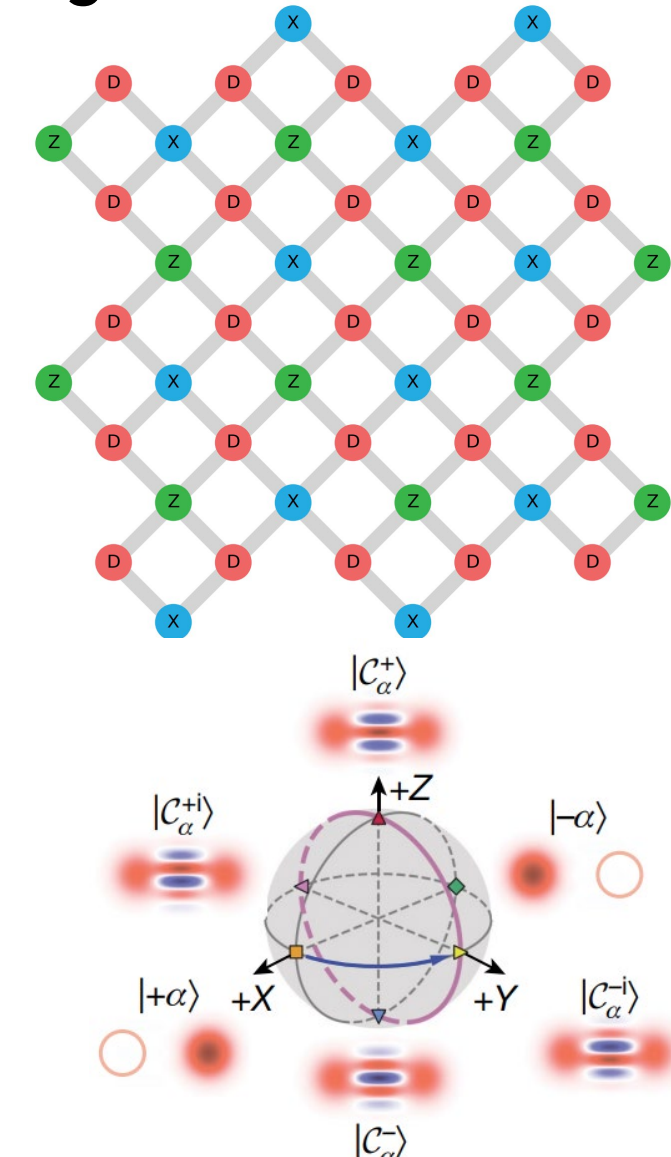


Fowler *et al.*, *Phys. Rev. A* **86**, 032324 (2012)

Quantum Error Correction with Superconducting Circuits

Approaches:

- Digital, qubit-based encodings: e.g. surface code, color code
- Continuous variable encodings in harmonic oscillator states: e.g. cat states, GKP states



Preskill, *Quantum* 2, 79 (2020)

Review: Terhal, *Rev. Mod. Phys.* 87, 307 (2015)

Bosonic Quantum Error Correction Experiments

Continuous QEC

- Dissipative-cat codes

Leghtas, et. al. Science 347, 853 (2015)

Lescanne, et. al. Nature Physics 16, 509 (2020)

Gertler et. al. Nature 590, 243 (2021)

- Kerr-cat codes

Grimm, et. al. Nature 584, 205 (2020)

Discrete QEC

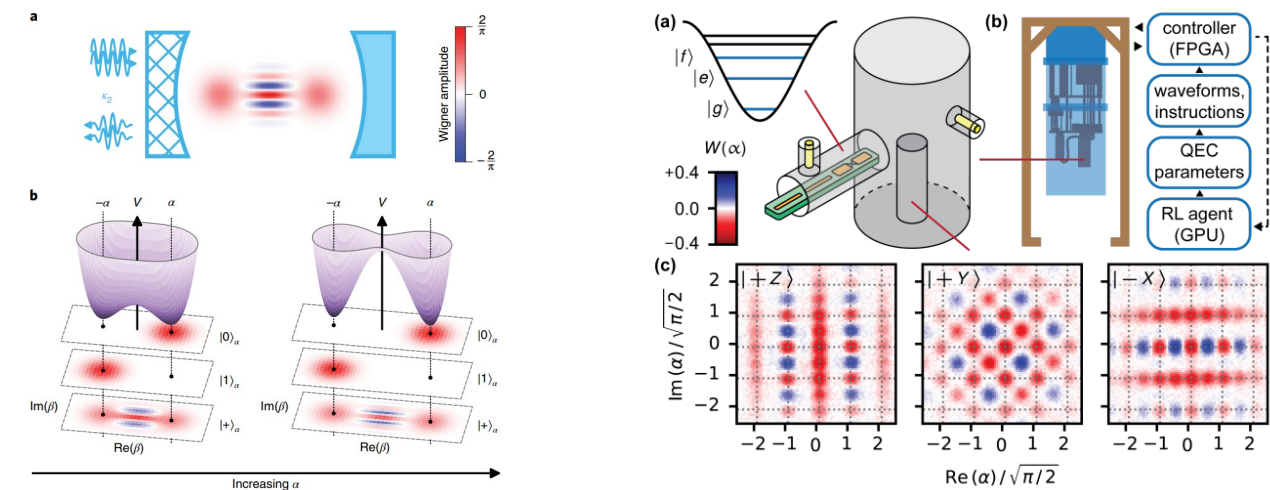
- Binomial bosonic codes

Ni, Z. et al., Nature 616, 56 (2023).

Hu et al., Nature Physics 15, 503 (2019).

- Cat-Codes

Ofek et. al., Nature 536, 441 (2016)



Lescanne et. al. Nat. Phys. 16, 509 (2020)

Sivak et. al. arXiv:2211.09116 (2022)

GKP codes

- Trapped ions

Flühmann et. al., Nature 566, 513 (2019)

de Neeve et. al., Nature Physics 18, 296 (2022)

- Superconducting circuits

Campagne-Ibarcq et. al., Nature 584, 368 (2020)

Sivak et al., Nature 616, 50 (2023).

The Challenge of Quantum Error Correction

Detect and correct two types of errors:

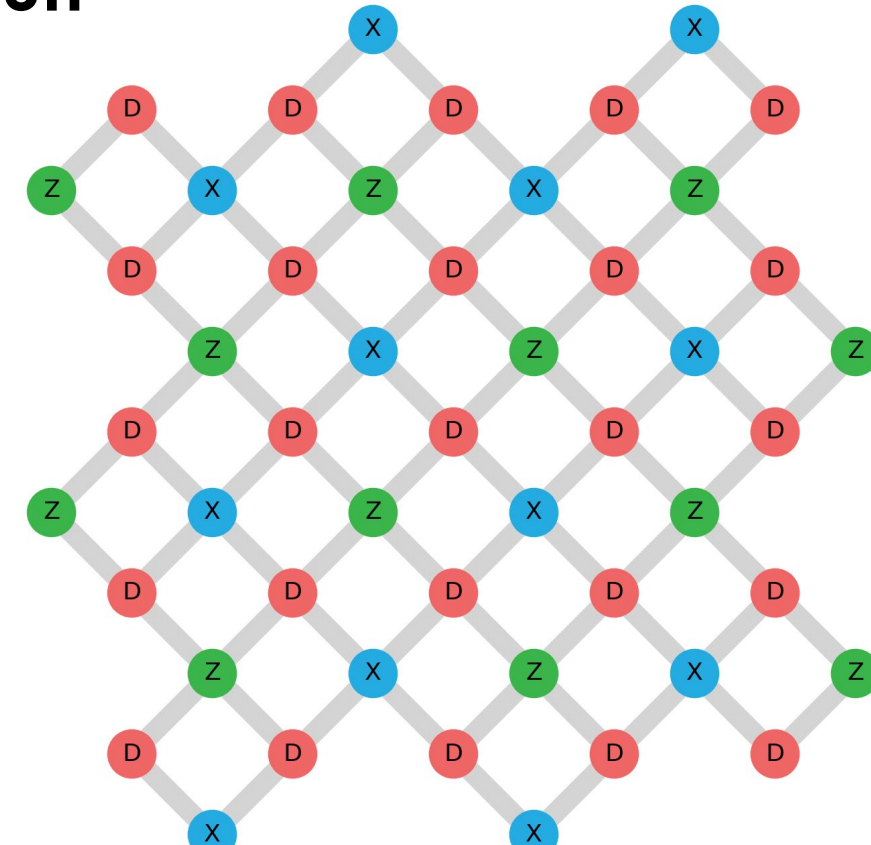
- Bit flips
- Phase flips

Preserve stored quantum states while detecting and correcting errors:

- Measurements collapse quantum (superposition) states

Solution: Use encoding

- Store **logical qubit** state $|\psi\rangle$ in a system of many **physical qubits**
- Make use of **symmetry properties (parity)** of logical qubit states
 - revealing errors ...
 - ... but not the encoded quantum state



Kitaev, *Annals of Physics* **303**, 2 (2003),
Dennis et al., *Journ. of Math. Physics* **43**, 4452 (2002)
Raussendorff, Harrington, *Phys. Rev. Lett.* **98**, 190504 (2007)
Fowler et al., *Phys. Rev. A* **86**, 032324 (2012)

The Surface Code – Main Features

Large error threshold $\epsilon_{\text{th}} \sim 1 \%$

- Logical error rate $\epsilon_L \propto (\epsilon_{\text{phys}}/\epsilon_{\text{th}})^{(d+1)/2}$

ϵ_{phys} : Physical error rate per step

ϵ_{th} : Threshold error rate

d : Distance of the code

Two-dimensional architecture

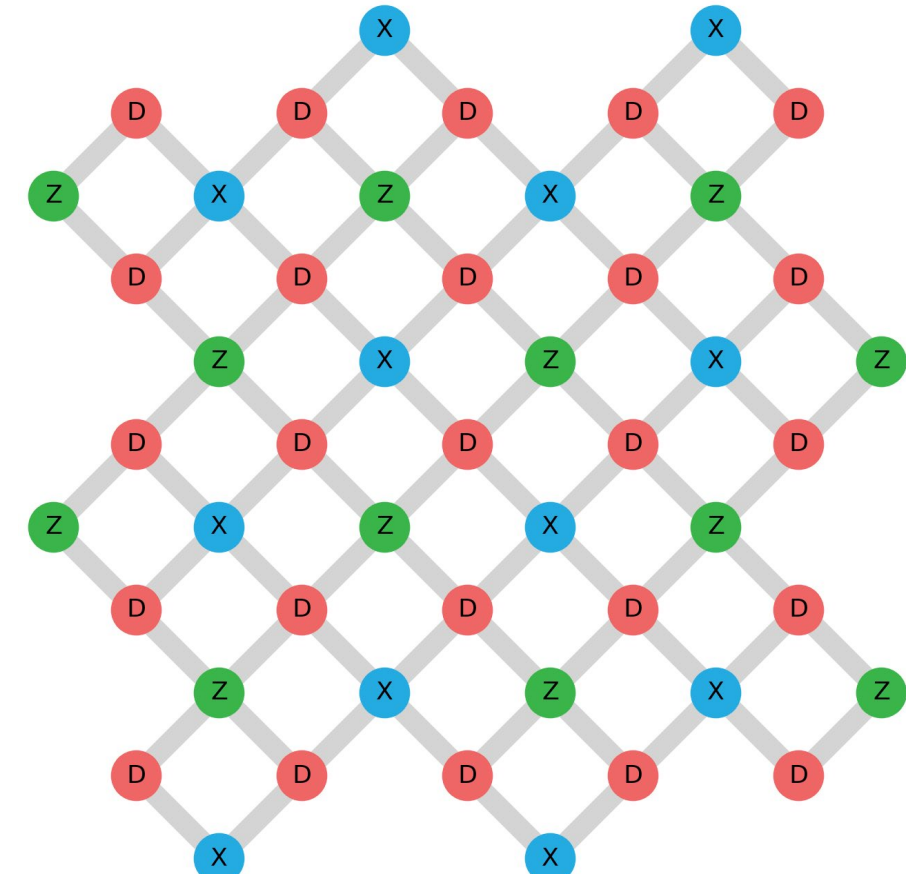
- All operations realizable on a planar qubit lattice
- Topological code: only local operations needed for error correction process

Kitaev, *Annals of Physics* **303**, 2 (2003),

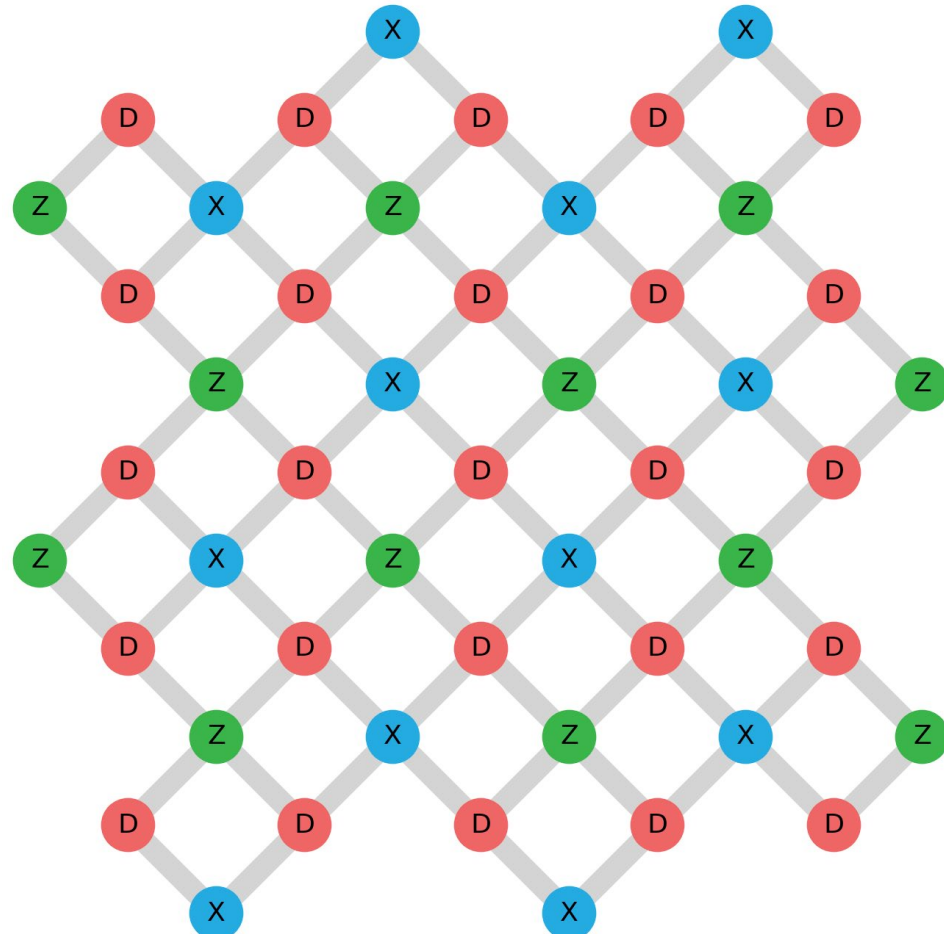
Dennis et al., *Journ. of Math. Physics* **43**, 4452 (2002)

Raussendorff, Harrington, *Phys. Rev. Lett.* **98**, 190504 (2007)

Fowler et al., *Phys. Rev. A* **86**, 032324 (2012)

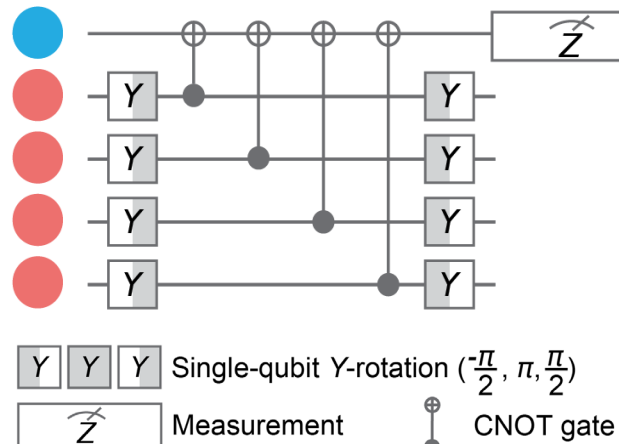


Elements of the Surface Code



Features:

- Two-dimensional ($d \times d$) grid of **data qubits**
- **X-type** and **Z-type** auxiliary qubits
- Auxiliary-qubit-assisted stabilizer measurement
 - $Z_1Z_2Z_3Z_4$ (or Z_1Z_2 at the edges)
 - $X_1X_2X_3X_4$ (or X_1X_2 at the edges)



Requirements:

- High-fidelity entangling gates between data and ancilla qubits
- Fast high-fidelity measurements of the ancilla qubits
- Low readout crosstalk between ancilla and data qubits
- Ability to do repeated gates and mid-cycle measurements

Fowler *et al.*, Phys. Rev. A **86**, 032324 (2012)

Versluis *et al.*, Phys. Rev. Applied **8**, 034021 (2017)

Distance-Two Surface Code for Error Detection

- Distance-two code: detect 1 error, correct 0 errors
- Stabilizers for parity measurement:

$$\underbrace{\hat{X}_1 \hat{X}_2 \hat{X}_4 \hat{X}_5, \quad \hat{Z}_1 \hat{Z}_4, \quad \hat{Z}_2 \hat{Z}_5}_{\text{Stabilizers commute, common eigenstates}}$$

- Logical eigenstates and their equal superpositions:

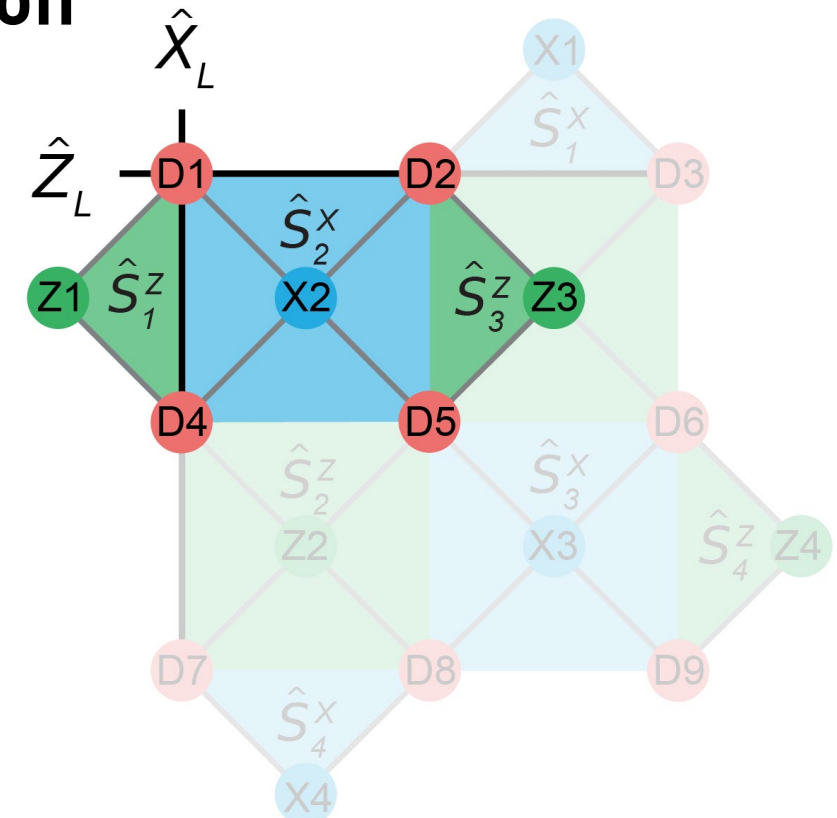
$$|0\rangle_L = \frac{1}{\sqrt{2}}(|0000\rangle + |1111\rangle)$$

$$|1\rangle_L = \frac{1}{\sqrt{2}}(|0101\rangle + |1010\rangle)$$

$$|+\rangle_L = \frac{1}{2}(|0000\rangle + |1111\rangle + |0101\rangle + |1010\rangle)$$

$$|-\rangle_L = \frac{1}{2}(|0000\rangle + |1111\rangle - |0101\rangle - |1010\rangle)$$

- Logical operators:
 - $\hat{X}_L = \hat{X}_1 \hat{X}_4$ or $\hat{X}_L = \hat{X}_2 \hat{X}_5$
 - $\hat{Z}_L = \hat{Z}_1 \hat{Z}_2$ or $\hat{Z}_L = \hat{Z}_4 \hat{Z}_5$
- Anti-commute with each other
and commute with stabilizers
(as needed for logical operators
in a stabilizer code)



Andersen *et al.*, *Nat. Phys.* **16**, 875 (2020)
 Chen *et al.*, *Nature* **595**, 7867 (2021)
 Marques *et al.*, *Nat. Phys.* **18**, 80 (2022)

Distance-Three Surface Code for Error Correction

Two-dimensional square lattice of qubits

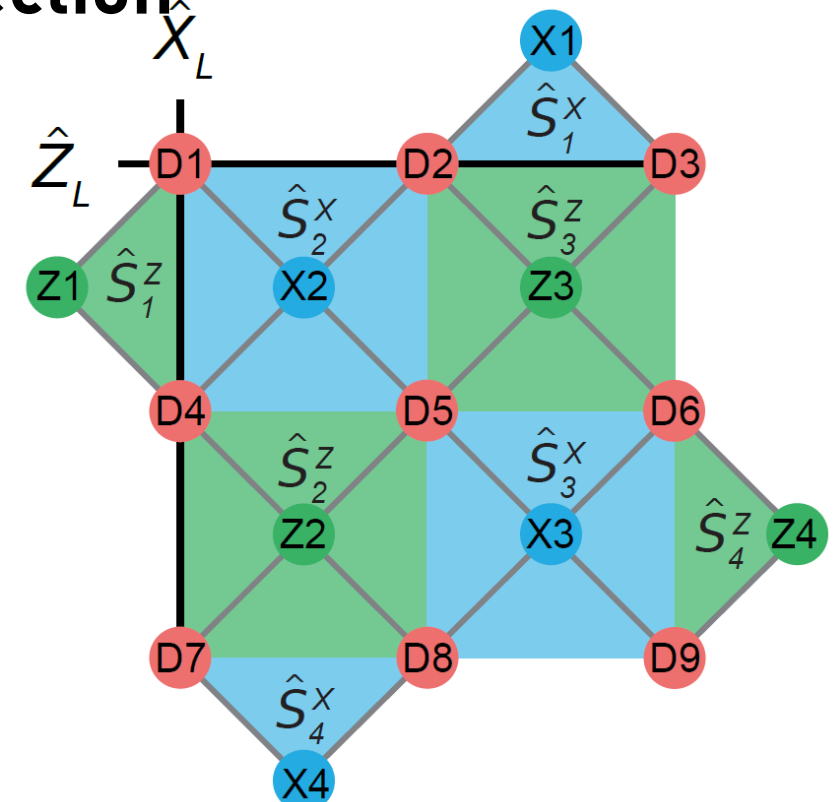
- $d^2 = 9$ Data qubits: encode single (logical) qubit
 - Logical operators: $\hat{Z}_L = \hat{Z}_1 \hat{Z}_2 \hat{Z}_3$ $\hat{X}_L = \hat{X}_1 \hat{X}_4 \hat{X}_7$
 - Distance d : min. number of Pauli operators in \hat{Z}_L, \hat{X}_L
 - Number of correctable errors: $\lfloor (d - 1)/2 \rfloor = 1$
- $d^2 - 1 = 8$ Auxiliary qubits: for parity measurements

Parity/Stabilizer measurements

- Detect errors without collapsing data-qubit state
(Stabilizer operators commute with \hat{Z}_L, \hat{X}_L)
- 4 Z-type Stabilizers \hat{S}^{Zi} to detect bit-flip errors
- 4 X-type Stabilizers \hat{S}^{Xi} to detect phase-flip errors

Bombin, Delgado, *Phys. Rev. A* 76, 012305 (2007)

Tomita, Svore, *Phys. Rev. A* 90, 062320 (2014)

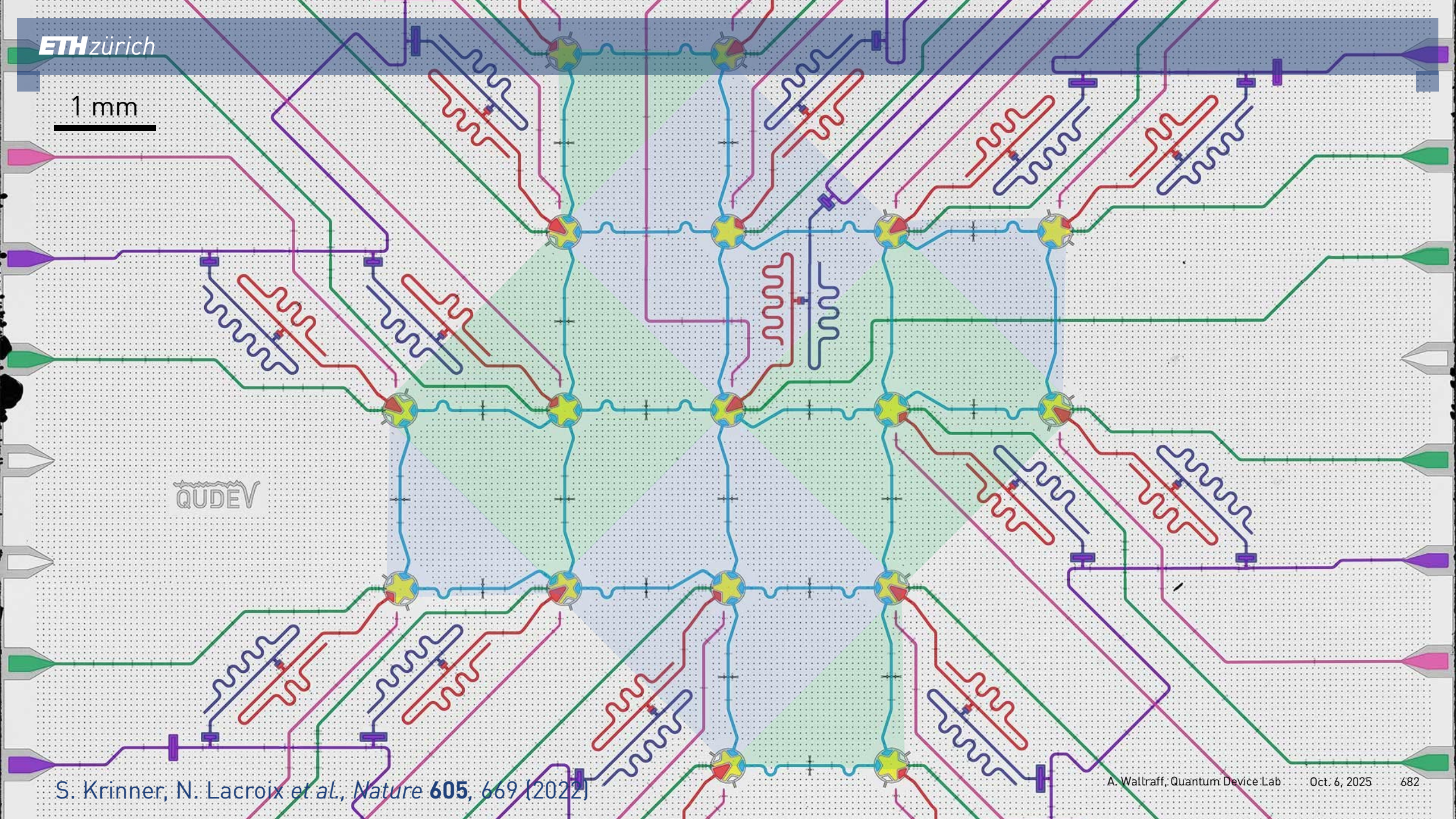


\hat{S}^{Z1}	$\hat{Z}_1 \hat{Z}_4$
\hat{S}^{Z2}	$\hat{Z}_4 \hat{Z}_5 \hat{Z}_7 \hat{Z}_8$
\hat{S}^{Z3}	$\hat{Z}_2 \hat{Z}_3 \hat{Z}_5 \hat{Z}_6$
\hat{S}^{Z4}	$\hat{Z}_6 \hat{Z}_9$

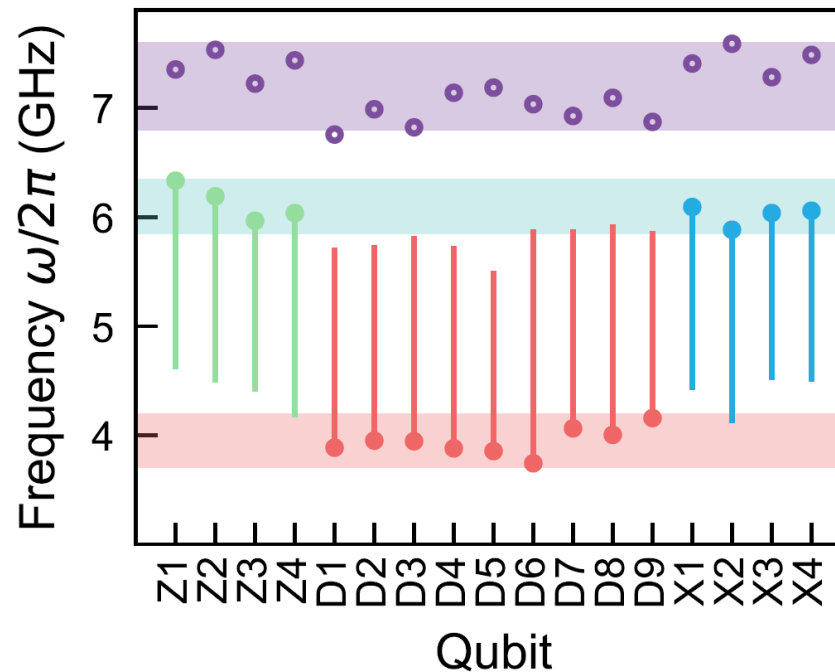
\hat{S}^{X1}	$\hat{X}_2 \hat{X}_3$
\hat{S}^{X2}	$\hat{X}_1 \hat{X}_2 \hat{X}_4 \hat{X}_5$
\hat{S}^{X3}	$\hat{X}_5 \hat{X}_6 \hat{X}_8 \hat{X}_9$
\hat{S}^{X4}	$\hat{X}_7 \hat{X}_8$

1 mm

QUDEV



Device Architecture



Frequency tunable qubits in two bands

- **Data qubits** at ~ 4 GHz
- **Auxiliary qubits** at ~ 6 GHz

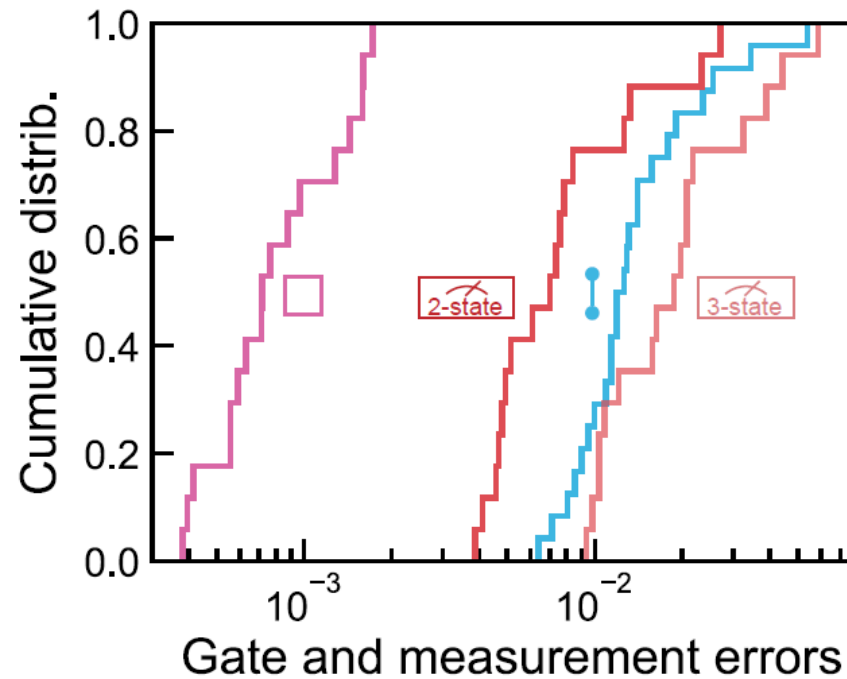
Features

- Small residual-ZZ couplings (≤ 8 kHz)
- Improved coherence using asymmetric SQUIDs creating upper and lower-frequency sweet spots
- Two-qubit CZ gates initiated by tuning both qubits
- Tuning range indicated by vertical bars
- Only auxiliary qubits evolve through $|2\rangle$ during a two-qubit gate

Readout resonators

- Single frequency band ~ 7 GHz

Device Performance



Averaged qubit coherence

- Energy relaxation time $T_1 \sim 33 \mu\text{s}$
- Ramsey decay time $T_2^* \sim 38 \mu\text{s}$

Single-qubit gates

- Mean gate error of $0.9(4) 10^{-3}$
- Duration of 40 ns

Two-qubit gates

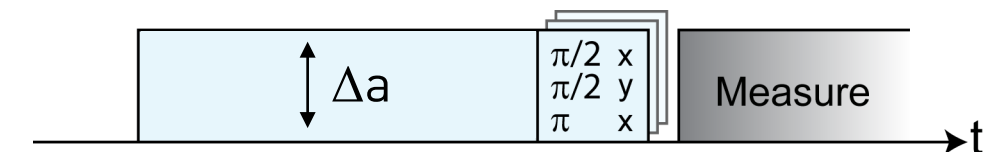
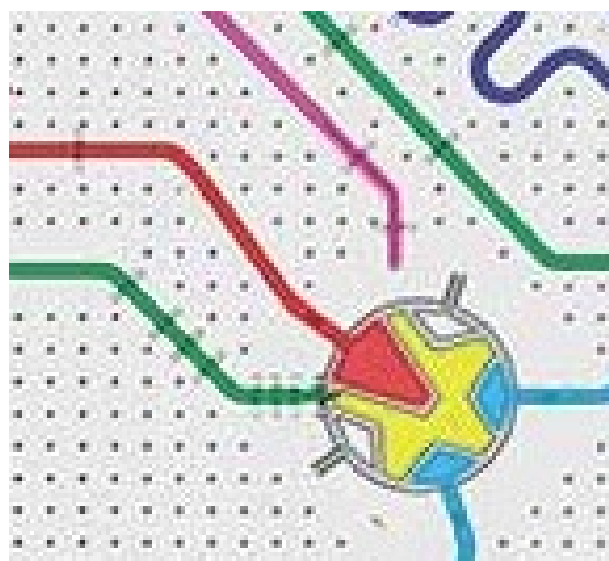
- Mean gate error of $15(10) 10^{-3}$
- Mean duration of $98(7)$ ns (including buffers)

Readout:

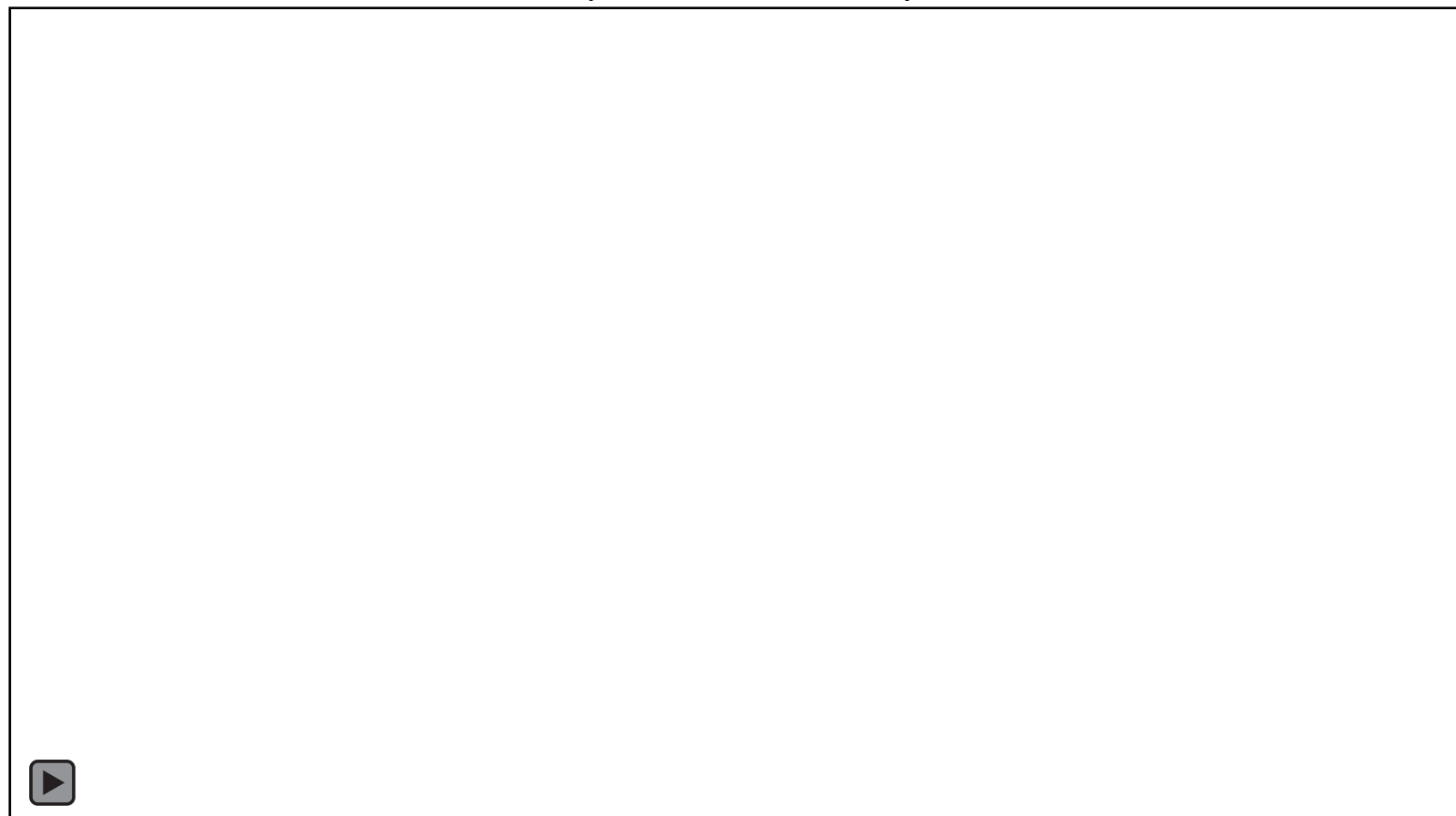
- Mean **two-state** assignment error: $9(7) 10^{-3}$
and **three-state** assignment error: $22(14) 10^{-3}$
- Duration: 300 ns (aux.) to 400 ns (data)

Controlling Single Qubits (Y Rotation)

- apply microwave pulse
- followed by read-out pulse
- both with controlled length, amplitude and phase
- Characterize gates by randomized benchmarking
- F > 99 %

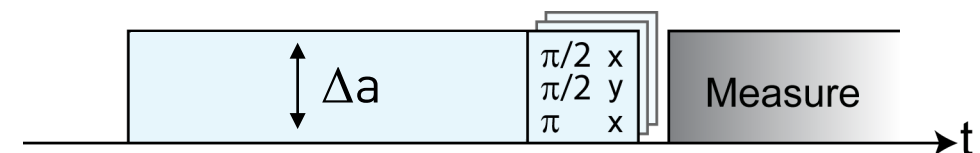


experimental density matrix and Pauli set:



Controlling Single Qubits (X Rotation)

- apply microwave pulse
- followed by read-out pulse
- both with controlled length, amplitude and phase
- Characterize gates by randomized benchmarking
- F > 99 %

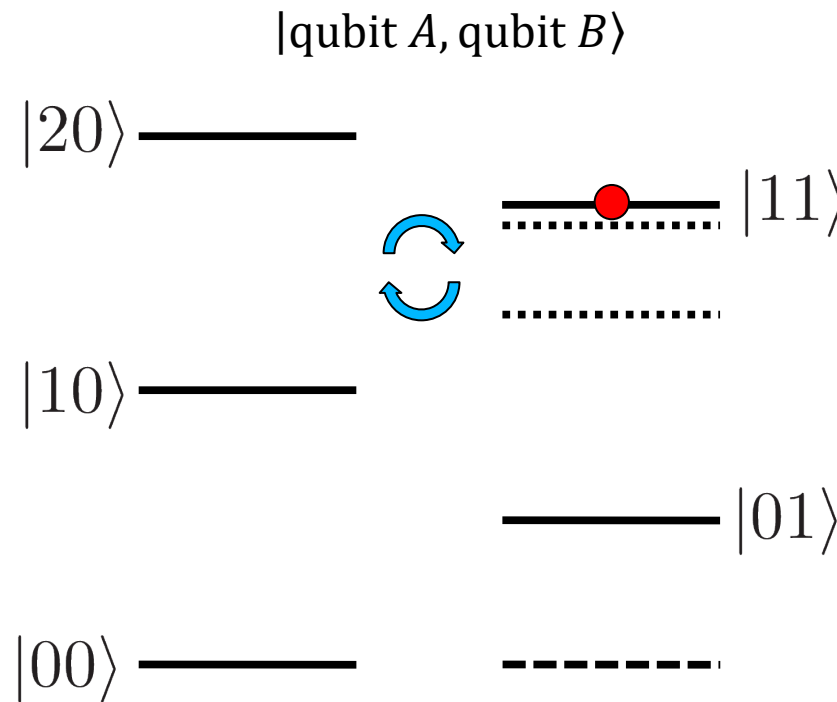


experimental density matrix and Pauli set:

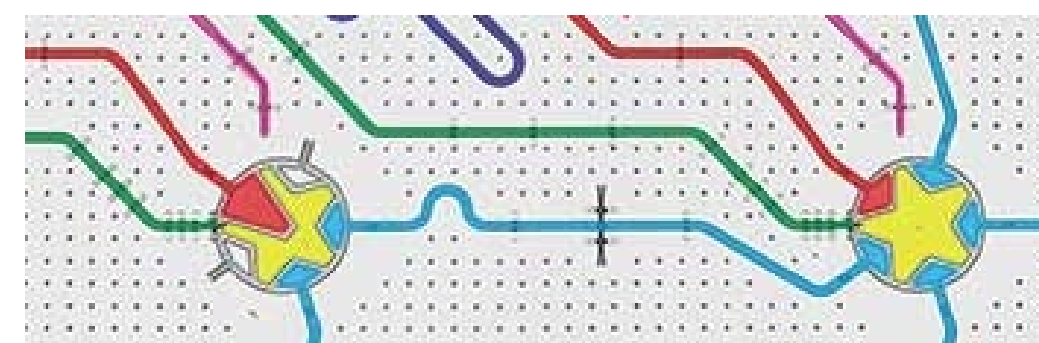


Universal Two-Qubit Controlled Phase Gate

Make use of qubit states beyond 0, 1



$$|11\rangle \longrightarrow i|20\rangle \longrightarrow -|11\rangle$$

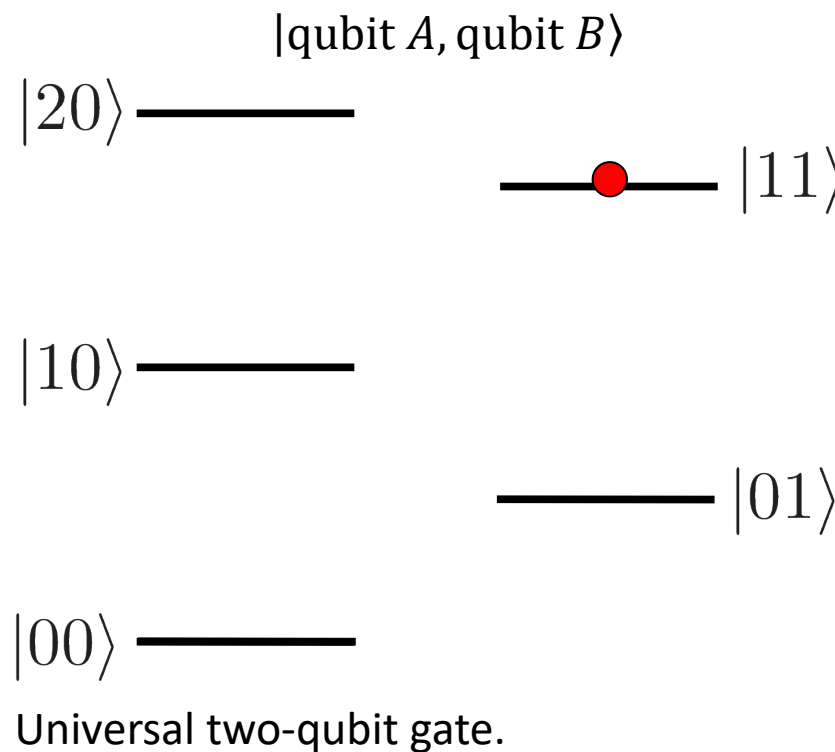


proposal: F. W. Strauch *et al.*, *Phys. Rev. Lett.* **91**, 167005 (2003).

first implementation: L. DiCarlo *et al.*, *Nature* **460**, 240 (2010).

Universal Two-Qubit Controlled Phase Gate

Make use of qubit states beyond 0, 1



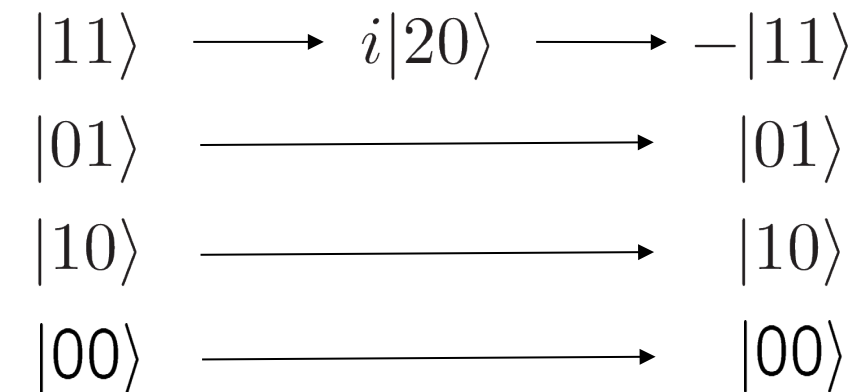
Universal two-qubit gate.

Test performance with process tomography or randomized benchmarking.

proposal: F. W. Strauch *et al.*, *Phys. Rev. Lett.* **91**, 167005 (2003).

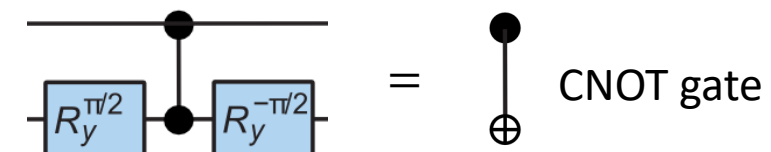
first implementation: L. DiCarlo *et al.*, *Nature* **460**, 240 (2010).

Qubits in states 01, 10 and 00 do not interact and thus acquire no phase shift



C-Phase gate:

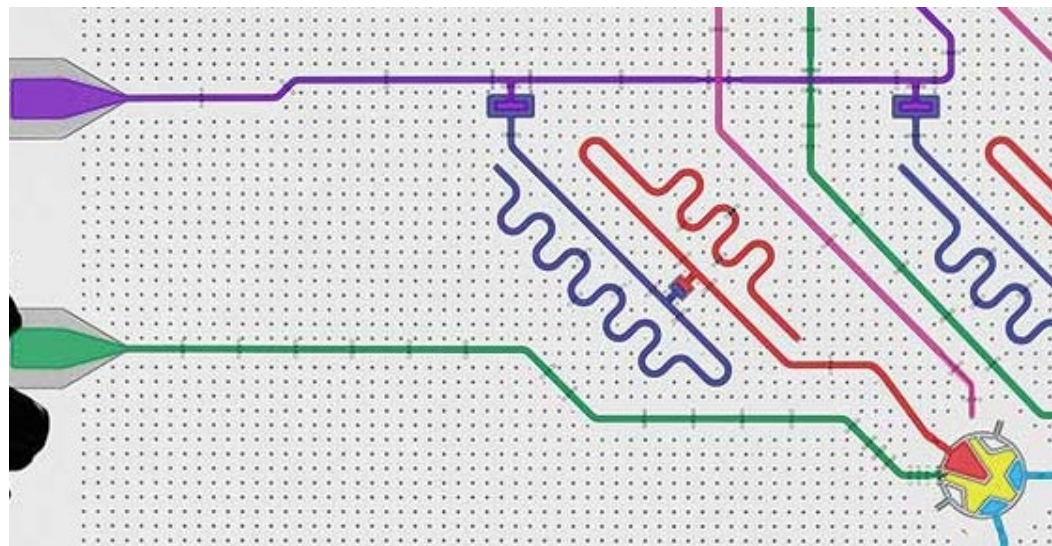
$$\begin{pmatrix} 1 & 0 & 0 & 0 \\ 0 & 1 & 0 & 0 \\ 0 & 0 & 1 & 0 \\ 0 & 0 & 0 & -1 \end{pmatrix}$$



Qubit Readout

Circuit design

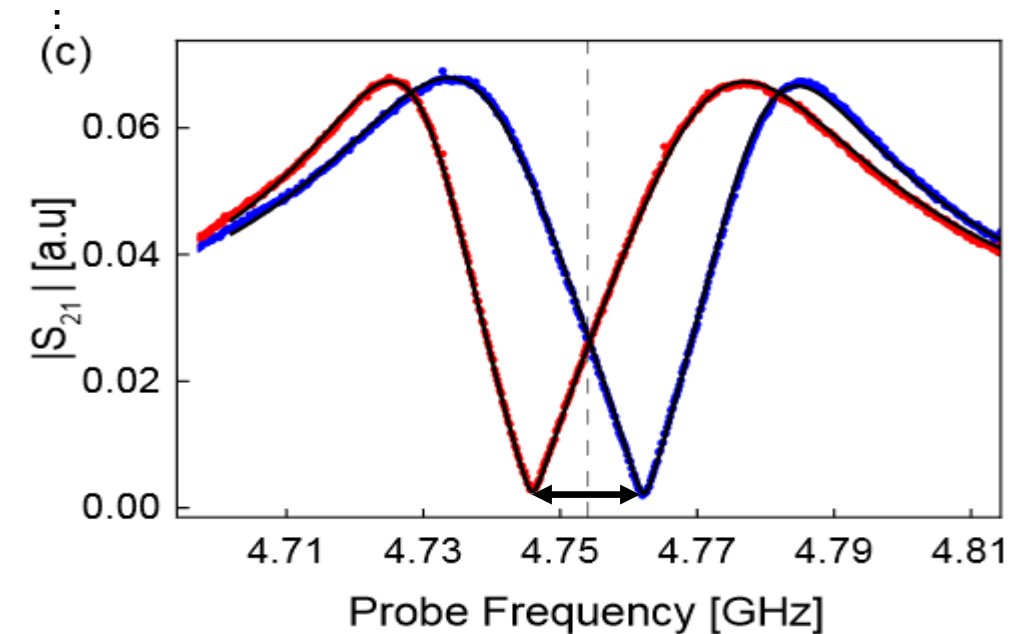
- $\lambda/4$ readout resonator & $\lambda/4$ Purcell filter



Performance

- F ~ 99.2 % at 88 ns integration time
- Optimized sample design
- Low-noise phase-sensitive JP-Amplifier

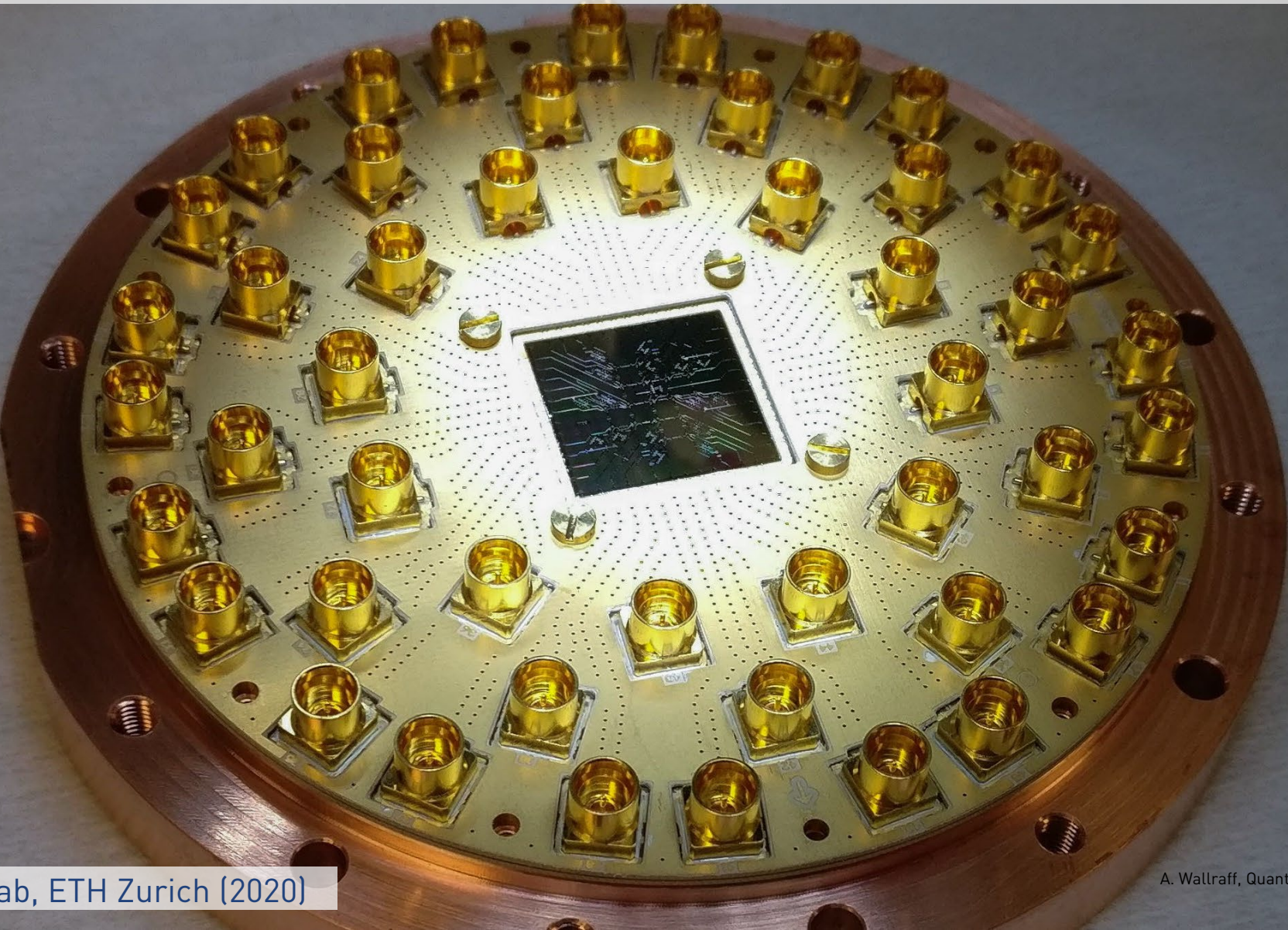
Transmission amplitude of readout circuit for qubit prepared in **ground (g)** or **excited (e)** state



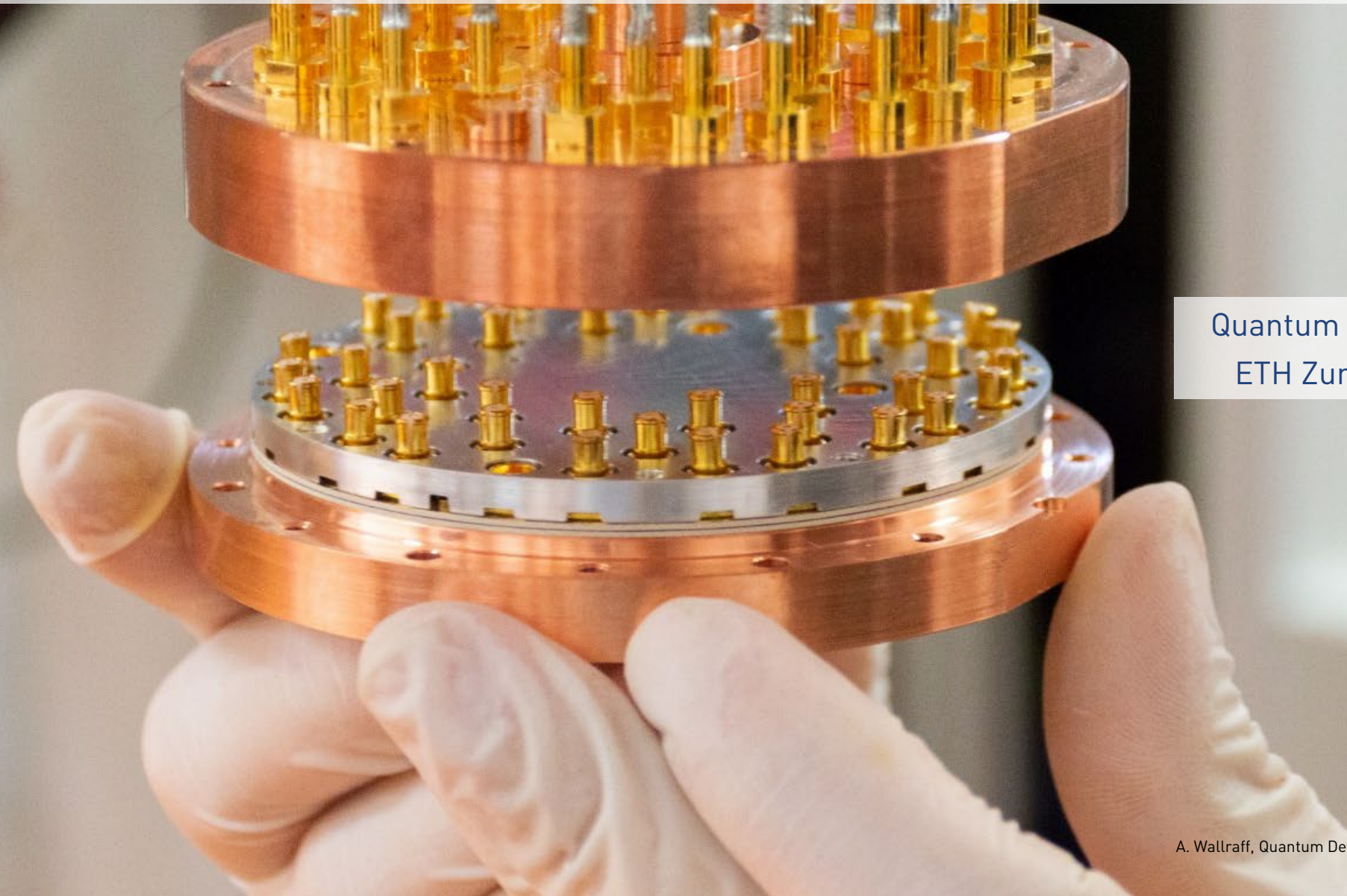
Features:

- large dispersive shift χ
- large resonator BW κ
- Purcell protection
- Low cross-talk when multiplexed

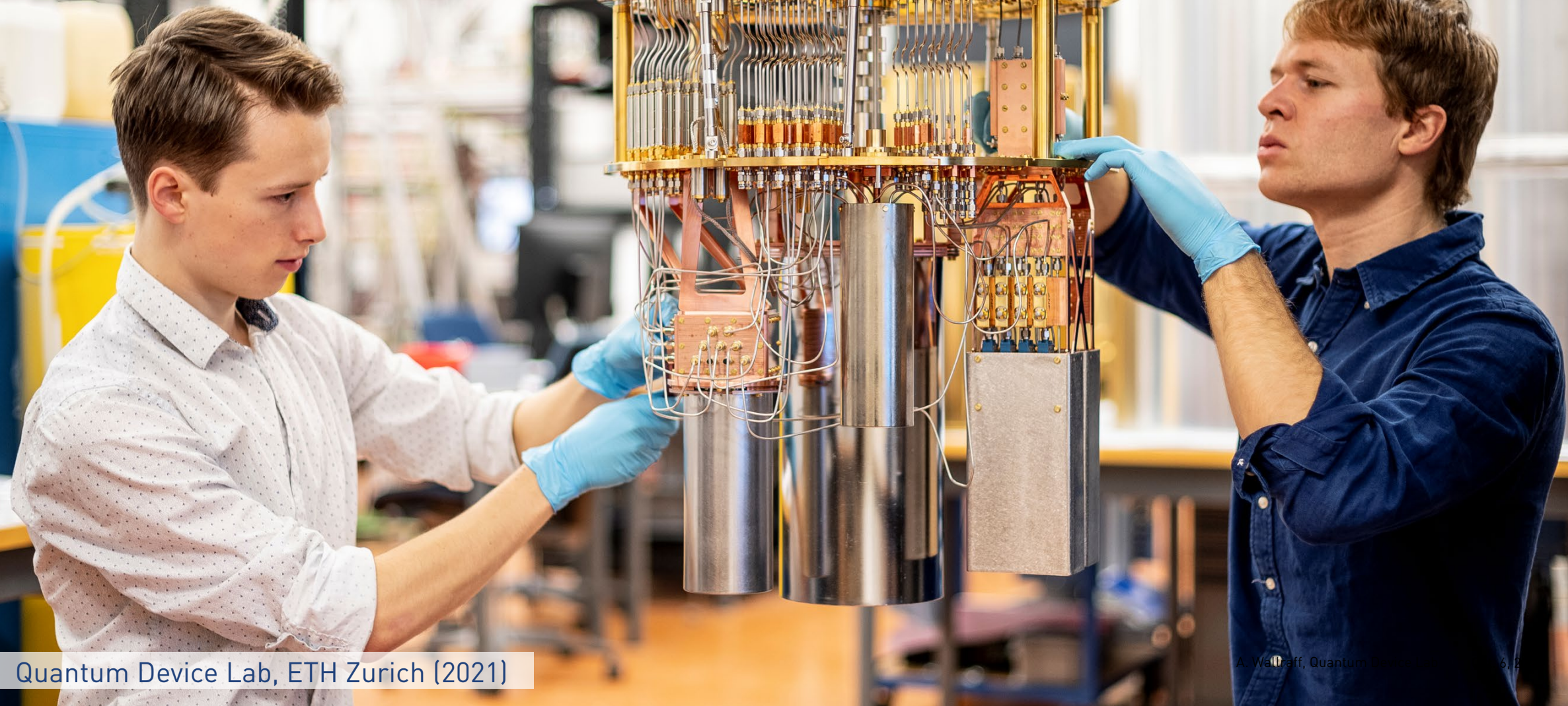
Distance-Three Surface-Code Device Mounted in Sample Holder



48-Port Sample Package (17-Qubit Device)



Quantum Device Lab,
ETH Zurich (2020)





Qubit-Encoded Quantum Error Correction Experiments

Bit or phase-flip codes (only X or Z errors):

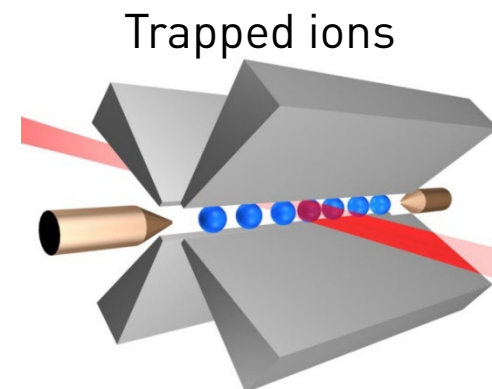
- NMR [Cory et al. Phys. Rev. Lett. 81, 2152 (1998)]
- Ions [Chiaverini et al. Nature 432, 602 (2004), Schindler et al. Science 322, 1059 (2011)]
- NV-Centers [Cramer et al. Nature Comm. 7, 11526 (2016)]
- Superconducting qubits [Riste et.al. Nature Comm. 6, 6983 (2015), Kelly et al. Nature 519, 66 (2015), Chen et al., Nature 595, 7867 (2021)]

Quantum codes, single-cycle experiments:

- Five-qubit code [Knill et al., PRL 86, 5811 (2001), Abobeih et al., arXiv:2108.01646 (2021)]
- Bacon-Shor code [Egan et al., Nature 598, 281 (2021)]

Repeated error detection in the surface code

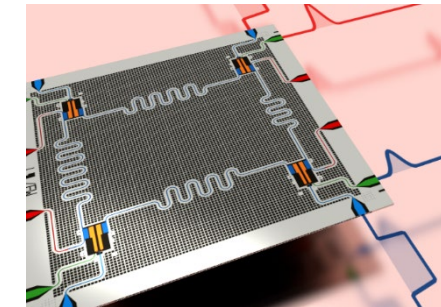
- Andersen et al., Nat. Phys. 16, 875 (2020)
- Chen et al., Nature 595, 7867 (2021)
- Marques et al., Nat. Phys. 18, 80 (2022)



Trapped ions

e.g. Blatt & Roos,
Nat. Phys. 8, 277 (2012)

Supercond. circuits



Picture: Y. Salathé
Review: e.g. Krantz et al., Appl. Phys. Rev. 6, 021318 (2019)

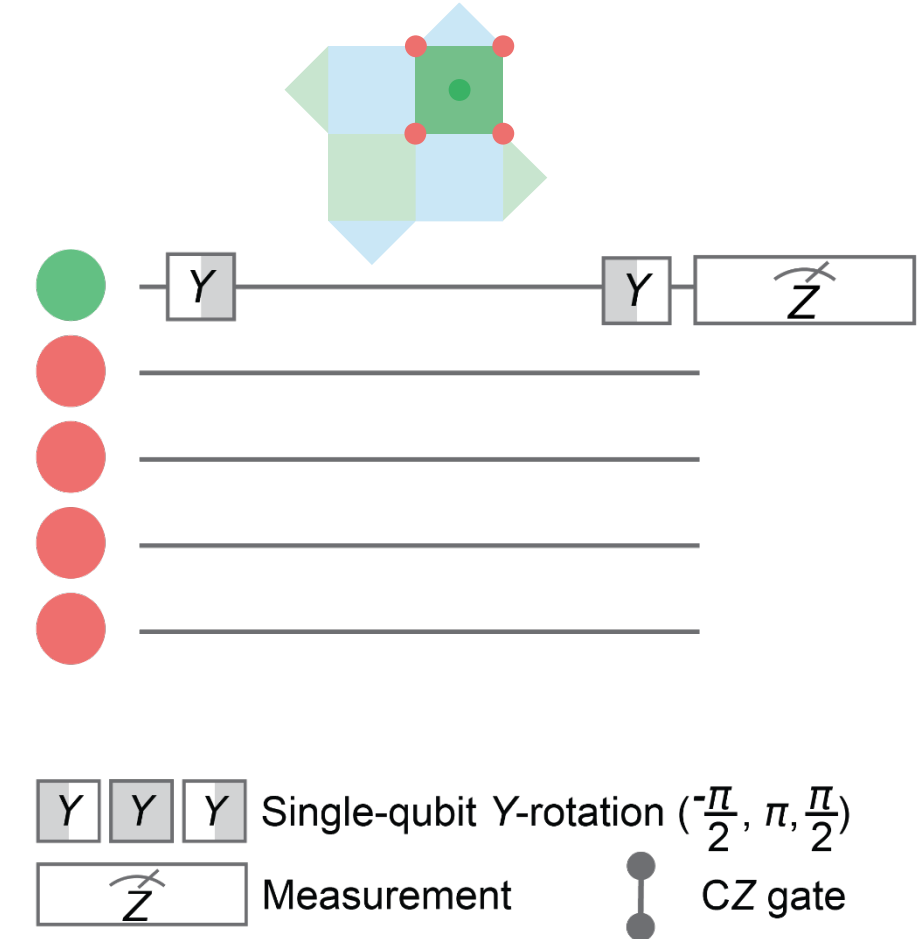
Repeated quantum error correction

- Color code (trapped ions)
Ryan-Anderson et al., PRX 11, 041058 (2021)
- Distance-3 surface code (s.c.)
Krinner, Lacroix et al., Nature 605, 669 (2022)
Zhao et al., PRL 129, 030501 (2022)
- Distance-3 heavy-hexagon code (s.c.)
Sundaresan et al., Nat. Commun. 14, 2852 (2023)
- Distance-3 to 5 scaling of the surface code (s.c.)
Google AI, Nature 614, 676 (2023)

Stabilizer Measurements

Quantum circuit

- Ramsey measurement on auxiliary qubit A_i

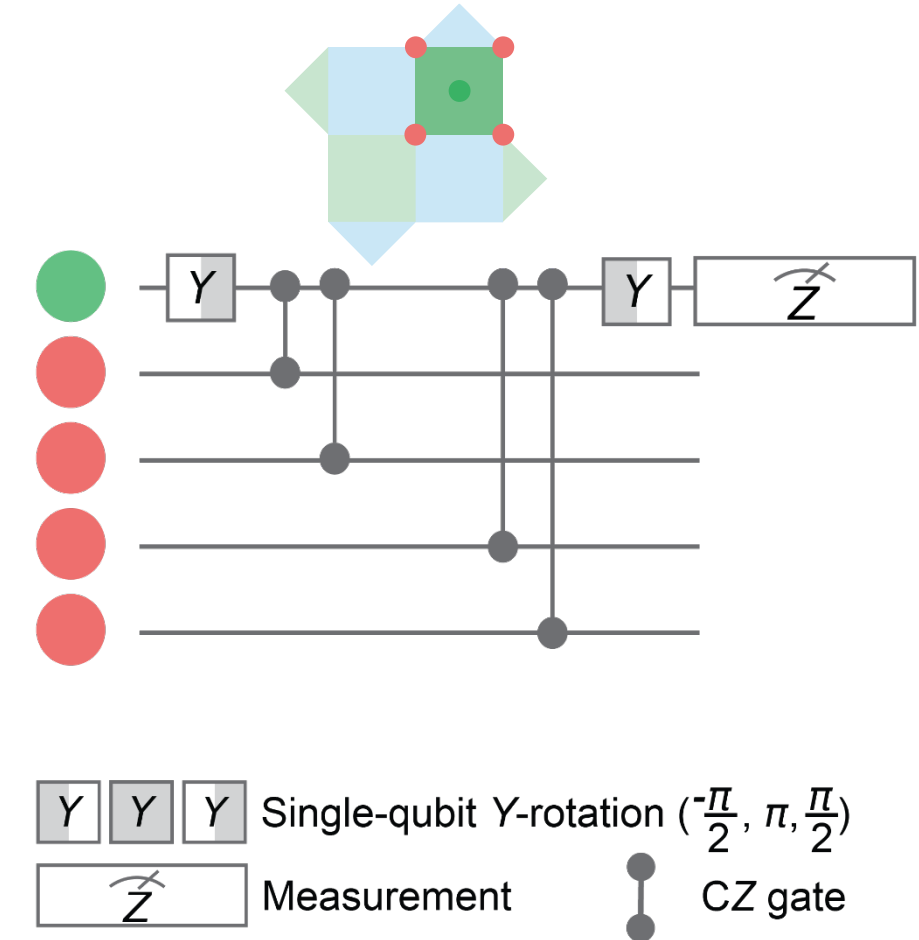


Stabilizer Measurements

Quantum circuit

- Ramsey measurement on auxiliary qubit Ai
- Controlled-phase (CZ) gates between Ai and four data qubits Dj
 - If Dj in $|1\rangle$: phase of Ai changes by π
- Resulting mapping:

Number of Dj in $ 1\rangle$:	Final phase of Ai	Final state of Ai	Stabilizer value s^{Ai}
Even	0	Unchanged	+1
Odd	π	Changed	-1



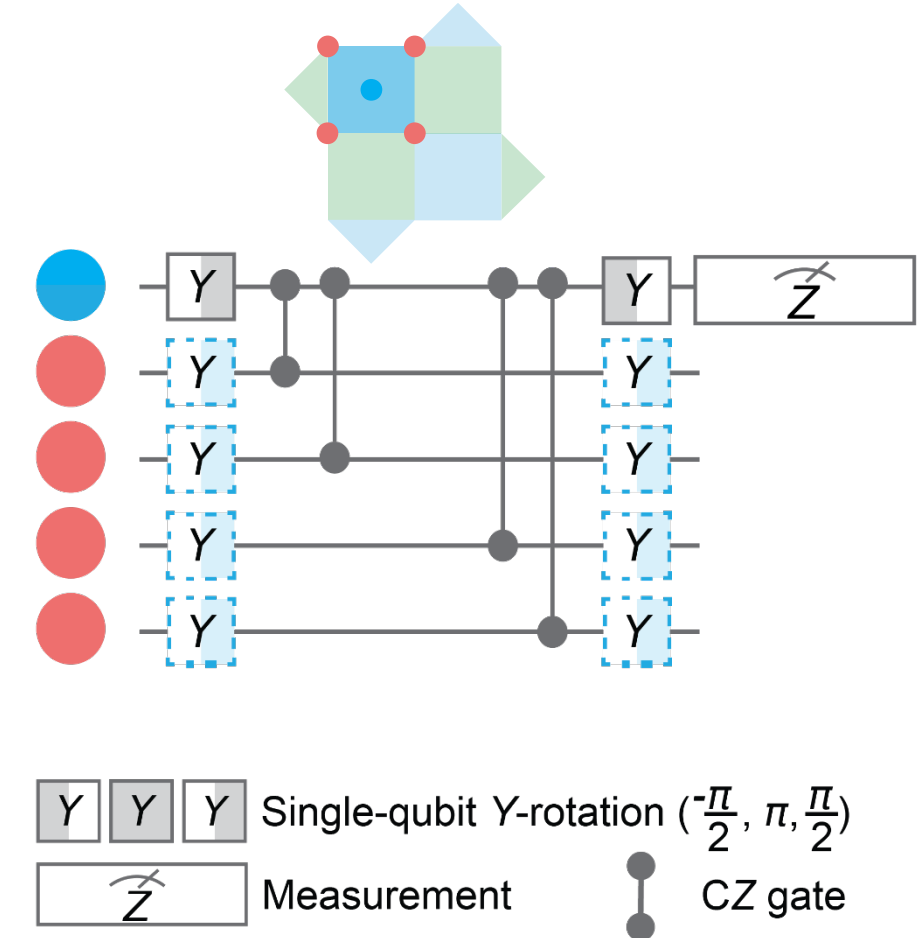
Stabilizer Measurements

Quantum circuit

- Ramsey measurement on auxiliary qubit Ai
- Controlled-phase (CZ) gates between Ai and four data qubits Dj
 - If Dj in $|1\rangle$: phase of Ai changes by π
- Resulting mapping:

Number of Dj in $ 1\rangle$:	Final phase of Ai	Final state of Ai	Stabilizer value s^{Ai}
Even	0	Unchanged	+1
Odd	π	Changed	-1

- X-type stabilizer with basis change on data qubits



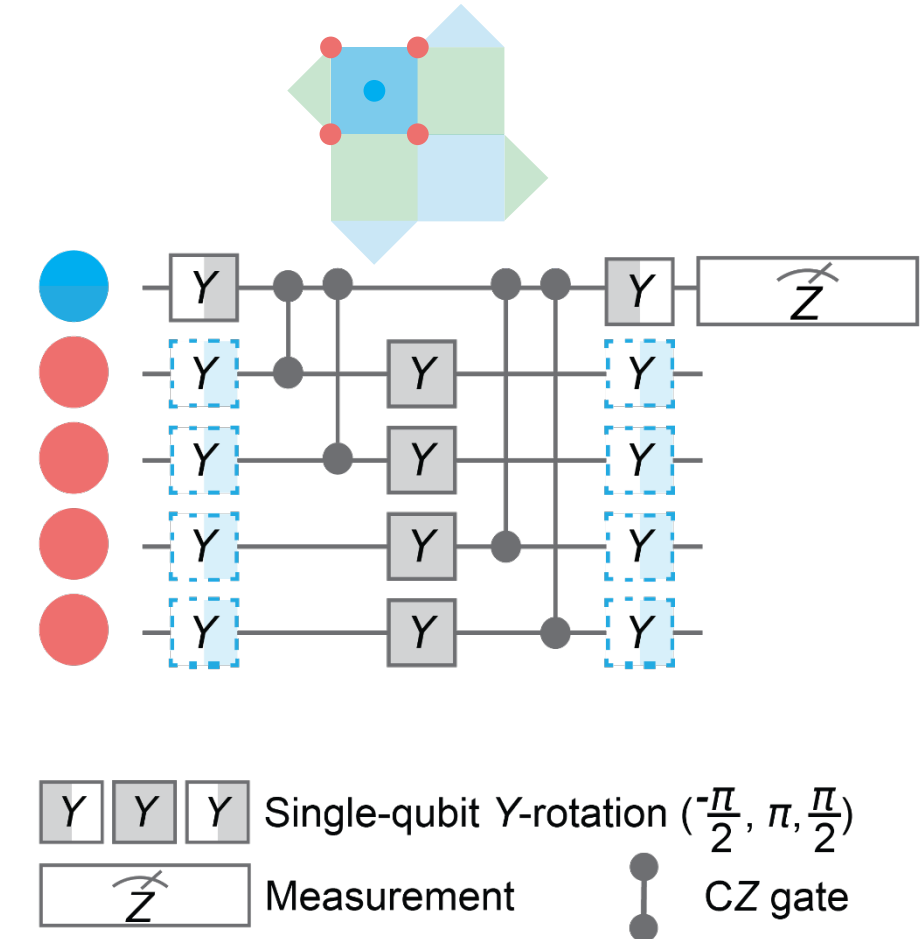
Stabilizer Measurements

Quantum circuit

- Ramsey measurement on auxiliary qubit Ai
- Controlled-phase (CZ) gates between Ai and four data qubits Dj
 - If Dj in $|1\rangle$: phase of Ai changes by π
- Resulting mapping:

Number of Dj in $ 1\rangle$:	Final phase of Ai	Final state of Ai	Stabilizer value s^{Ai}
Even	0	Unchanged	+1
Odd	π	Changed	-1

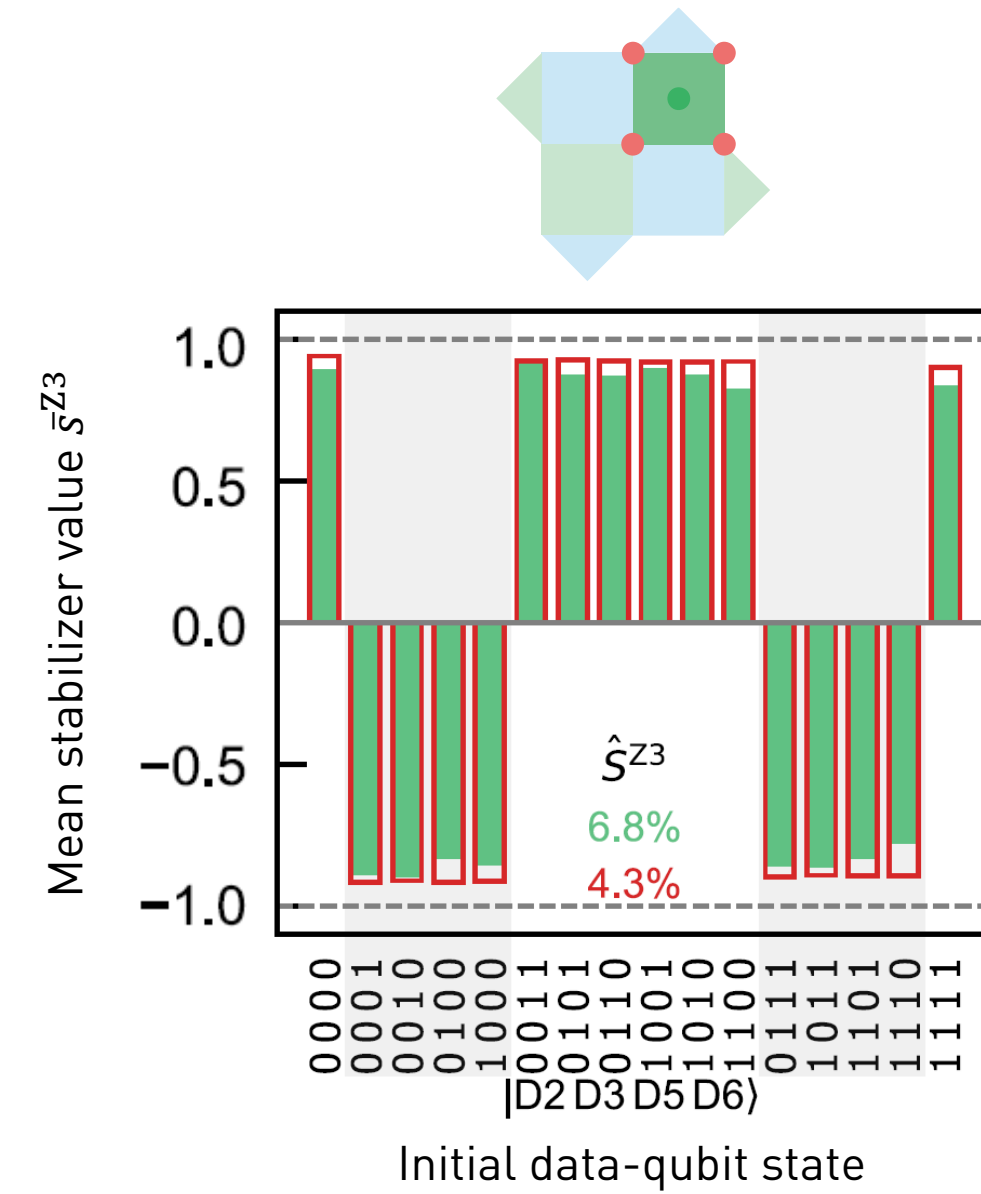
- X-type stabilizer with basis change on data qubits
- Echo pulses on data qubits to reduce both
 - Dephasing
 - Residual coherent coupling to spectator qubits



Stabilizer Characterization

Individual characterization

- Prepare data qubits of plaquette in all 4 (weight-2) or 16 (weight-4) basis states
- Stabilizer execution yields $s^{Ai} = \pm 1$
- Average over $\sim 4 \times 10^4$ measurements to obtain \bar{s}^{Ai}
- **Measured** and **calculated** error



Stabilizer Characterization

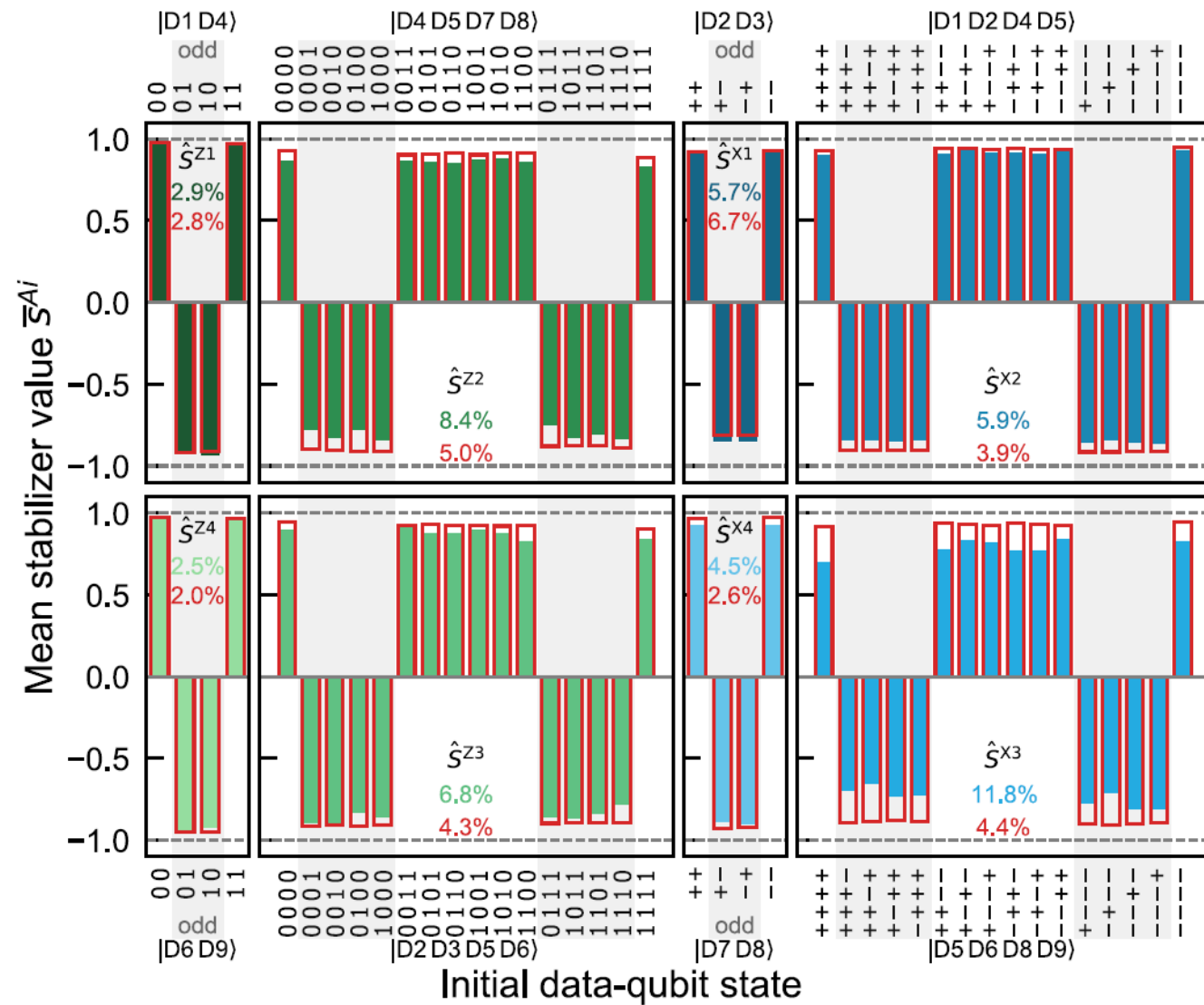
Individual characterization

- Prepare data qubits of plaquette in all 4 (weight-2) or 16 (weight-4) basis states
- Stabilizer execution yields $s^{Ai} = \pm 1$
- Average over $\sim 4 \times 10^4$ measurements to obtain \bar{s}^{Ai}
- **Measured** and **calculated** error

Average parity error

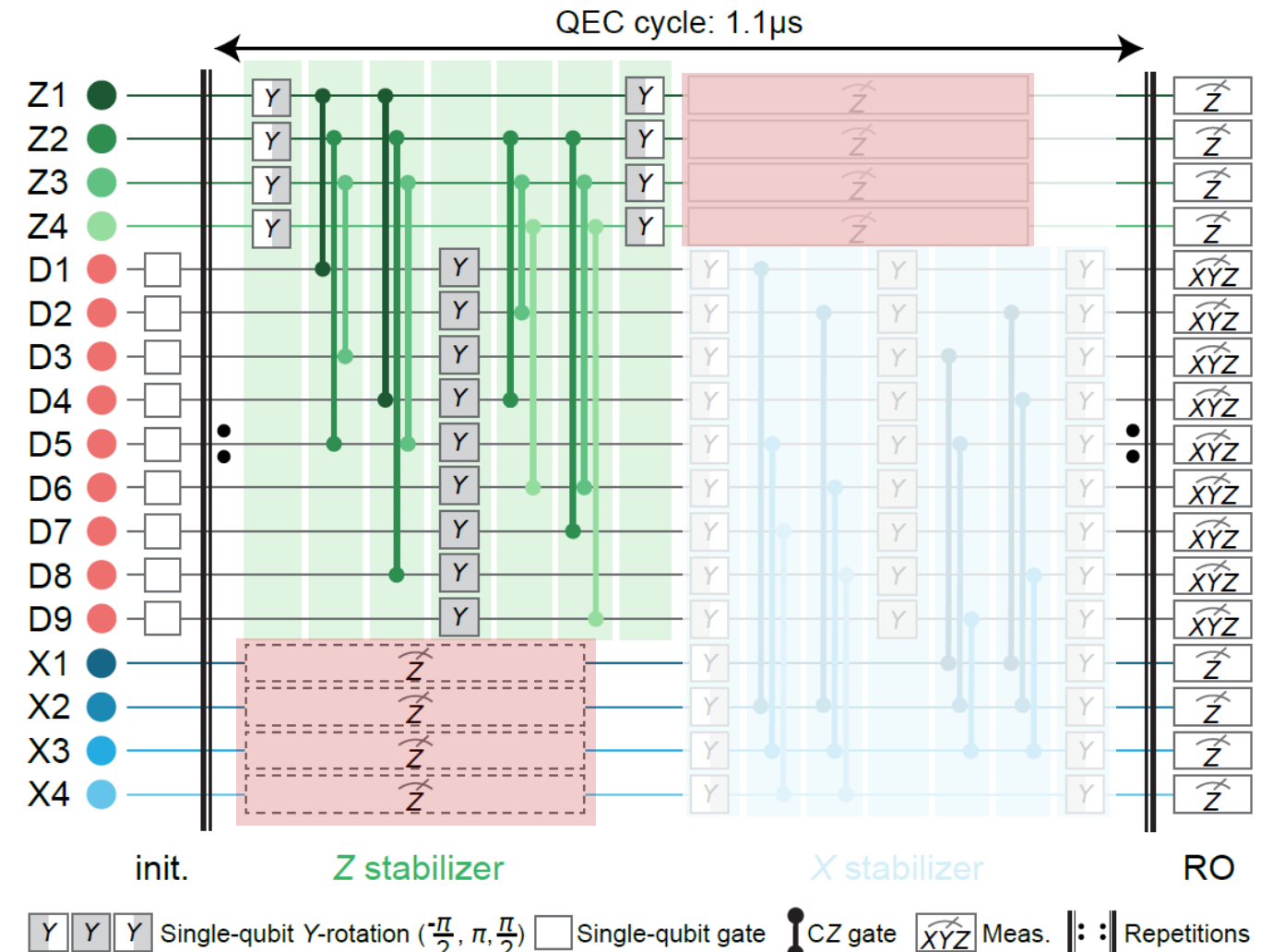
- Weight-2 stabilizers: 3.9(1.3) %
- Weight-4 stabilizers: 8.2(2.2) %

Qualitative agreement with **master-equation simulations**



The Surface Code Cycle

- All four \hat{S}^{Zi} measured in parallel
- All four \hat{S}^{Xi} measured in parallel
- Pipelining: **Read out** one stabilizer type while running gates of the other.
- Logical state preparation: $|0\rangle_L$, $|1\rangle_L$ and $|\pm\rangle_L = (|0\rangle_L \pm |1\rangle_L)/\sqrt{2}$ in single cycle.
- State preservation over n cycles
 - Cycle duration: 1.1 μ s
 - Leakage detection and rejection executed in every cycle
 - circuits with ~ 800 single-qubit gates and ~ 400 two-qubit gates



Versluis et al., PR Applied 8, 034021 (2017)

S. Krinner, N. Lacroix et al., Nature 605, 669 (2022)

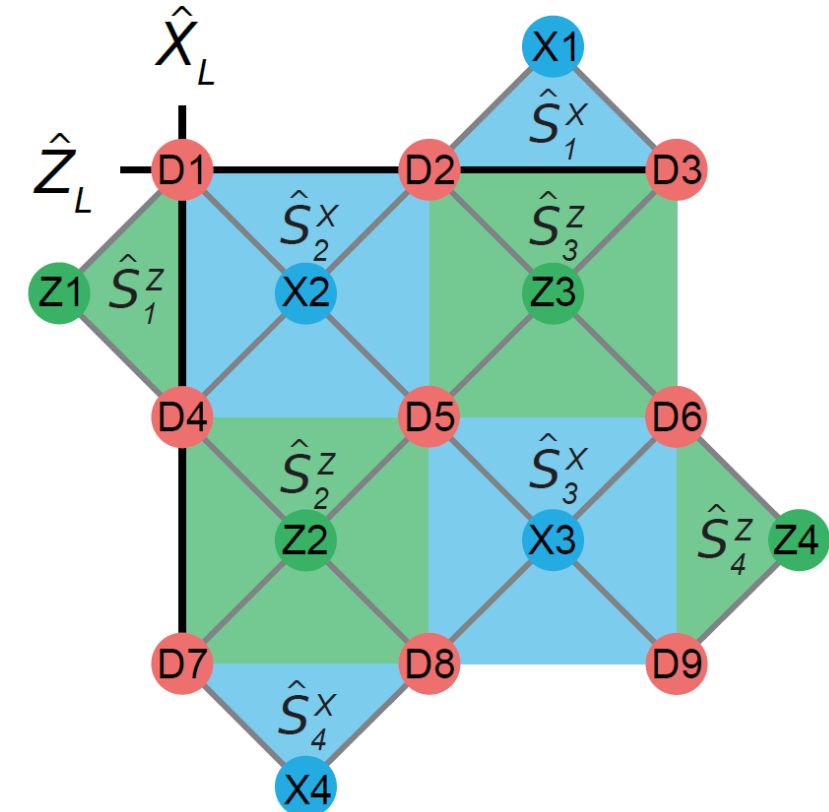
Repeated Quantum Error Correction

Measurement of Logical Z and Logical X Operators

- Initialization
 - $|0\rangle_L$: prepare data qubits in $|0\rangle^{\otimes 9}$
 - $|1\rangle_L$: prepare data qubits in $X_L|0\rangle^{\otimes 9}$
 - $|+\rangle_L$: prepare data qubits in $|+\rangle^{\otimes 9}$
 - $|-\rangle_L$: prepare data qubits in $Z_L|+\rangle^{\otimes 9}$
- Perform n QEC cycles
- Read out all data qubits in Z-basis (X-basis)

Analysis

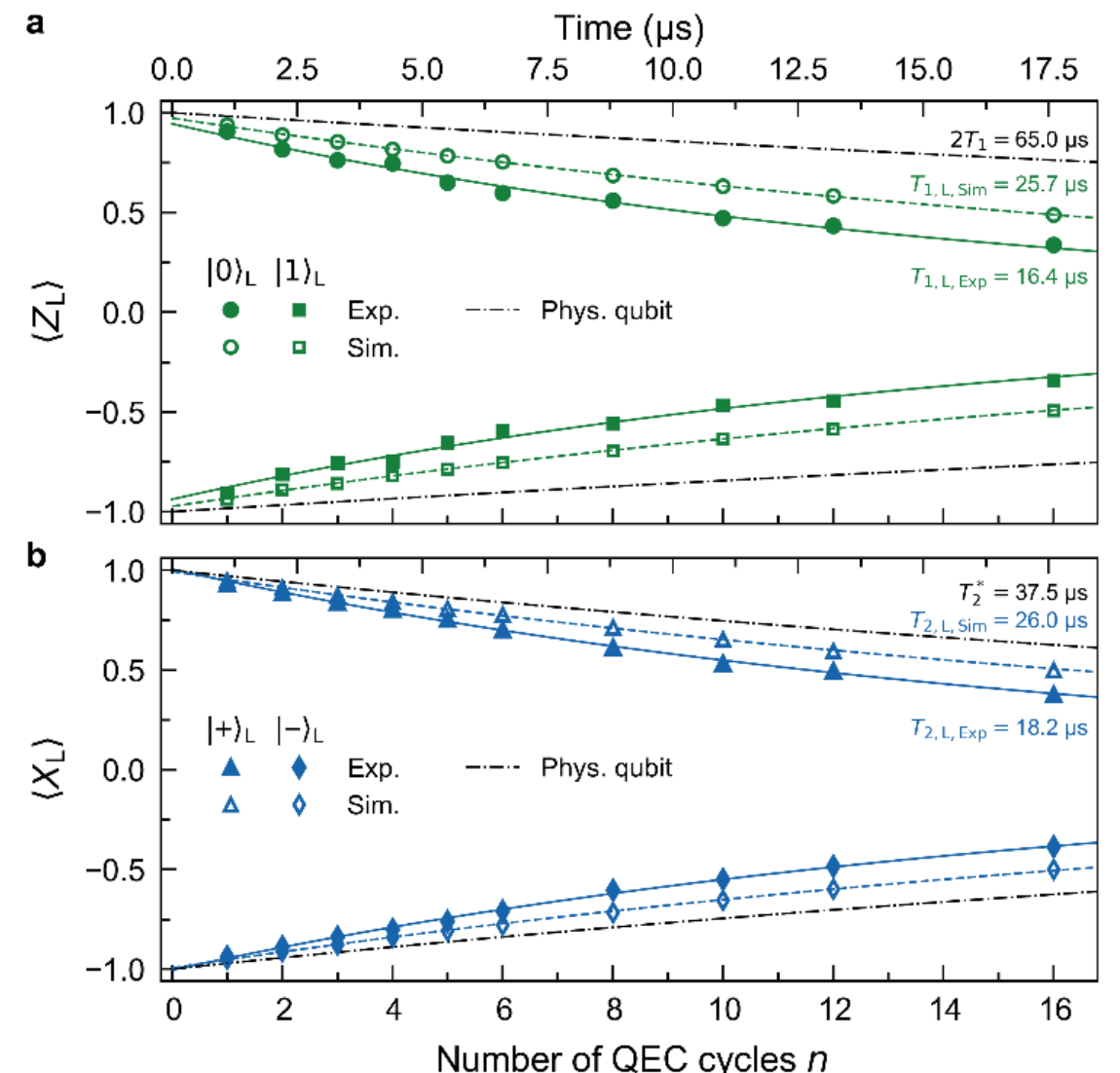
- Determine logical operator $z_L = z_1 z_2 z_3 = \pm 1$ ($x_L = x_1 x_4 x_7 = \pm 1$) for each run with up to n repeated cycles
- Apply correction conditioned on decoded syndromes for each run
- Average over runs with n repeated cycles to compute $\bar{z}_L = \langle \hat{Z}_L \rangle$ ($\bar{x}_L = \langle \hat{X}_L \rangle$)



Repeated Quantum Error Correction

Outcomes Logical Z and Logical X

- Exponential decay of logical expectation values
- Logical lifetime
 $T_{1,L} = 16.4(8) \mu\text{s} \gg t_c = 1.1 \mu\text{s}$
- Logical coherence time
 $T_{2,L} = 18.2(5) \mu\text{s} \gg t_c = 1.1 \mu\text{s}$
- Master equation simulation of logical lifetimes of $\sim 26 \mu\text{s}$ provide upper bound for achievable lifetimes with our device performance
- Physical coherence time $\bar{T}_2^* = 37.5 \mu\text{s} > T_{2,L}$
- Twice physical lifetime $2\bar{T}_1 = 65.0 \mu\text{s} > T_{1,L}$



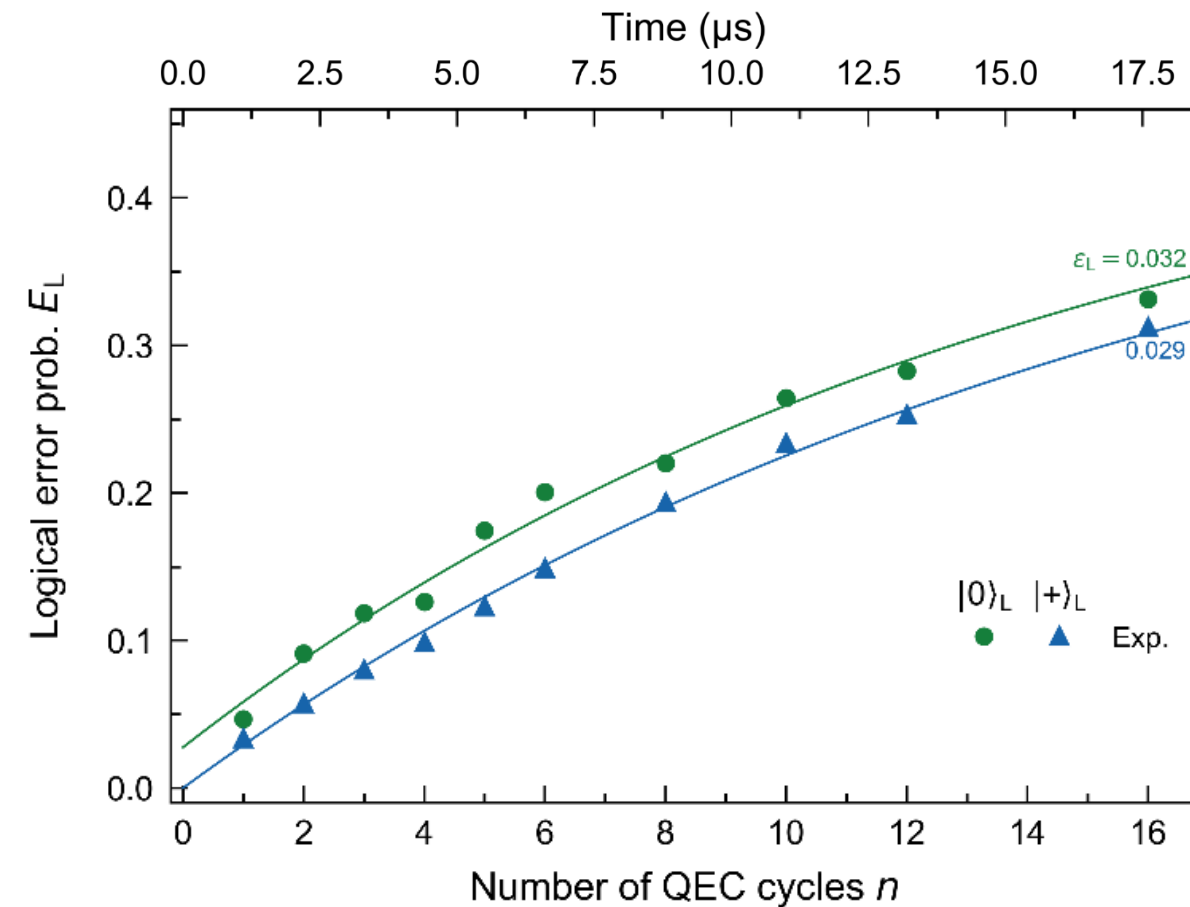
Logical Error Probability and Logical Error per Cycle

Logical error probability:

- $E_L = (1 - \langle \hat{Z}_L \rangle)/2$ for eigenstates of \hat{Z}_L
- $E_L = (1 - \langle \hat{X}_L \rangle)/2$ for eigenstates of \hat{X}_L

Logical error per cycle:

- Extracted from fit to $E_L(n)$ or from $T_{1/2,L}$:
- $$\epsilon_L = \frac{1}{2} [1 - \exp(-t_c/T_{1/2,L})] \approx t_c/2T_{1/2,L}$$
- $\epsilon_L \sim 0.03$



Repeated Quantum Error Correction with $d \geq 3$ Codes

Published work:

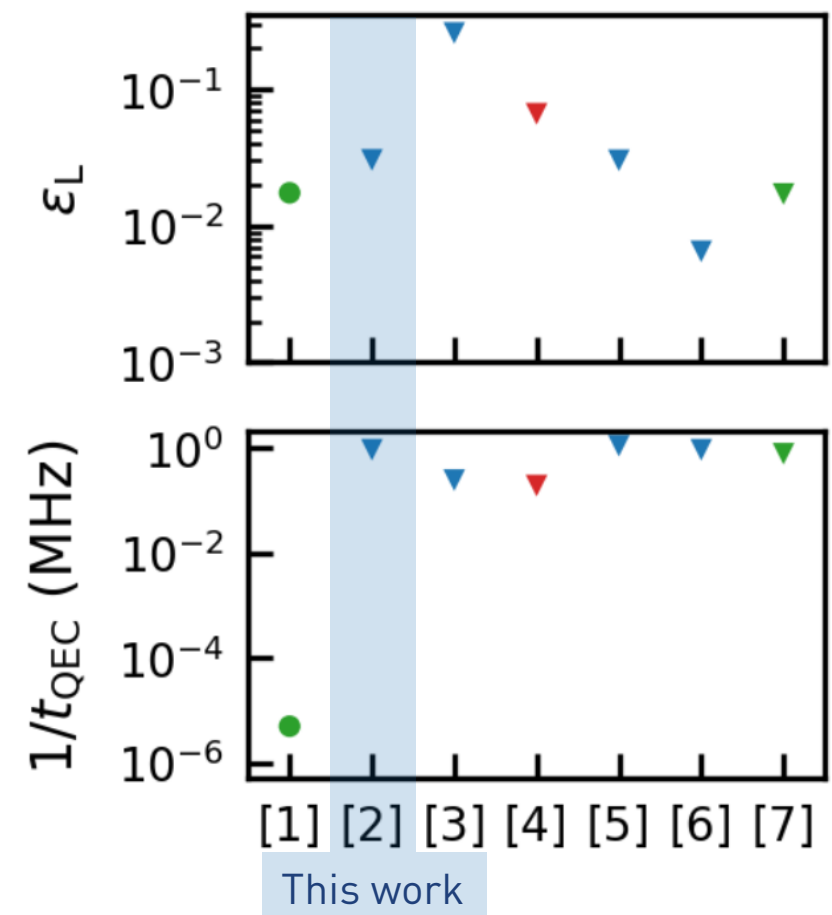
- Honeywell: [1] Ryan-Anderson *et al.*, *Phys. Rev. X* **11**, 041058 (2021)
- ETHZ: [2] Krinner, Lacroix *et al.* *Nature* **605**, 669 (2022)
- USTC: [3] Zhao *et al.*, *PRL* **129**, 030501 (2022)
- IBM: [4] Sundaresan *et al.*, *Nat. Commun.* **14**, 2852 (2023)
- Google: [5] Google Quantum AI, *Nature* **614**, 676 (2023)
- Google: [6] Google Quantum AI, *Nature* **638**, 920 (2025)
- Google: [7] Lacroix *et al.*, *Nature* (2025)

Implementations:

- superconducting-circuits (∇) and trapped-ions (\circ)
- Color code, surface code and heavy-hexagon code

Performance criteria

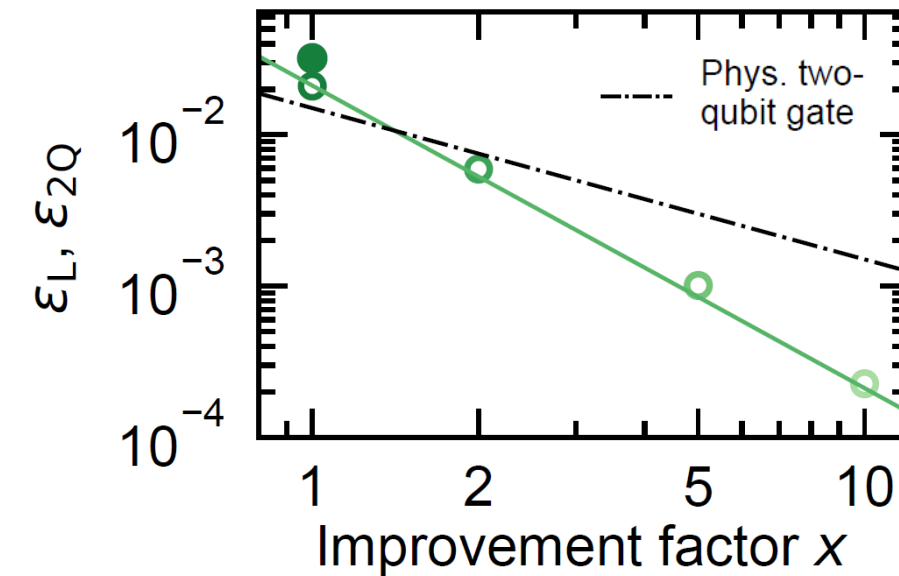
- Small logical error per cycle ϵ_L
- High QEC cycle rate $1/t_{\text{QEC}}$



Performance Assessment and Projection

Two-qubit-gate break-even

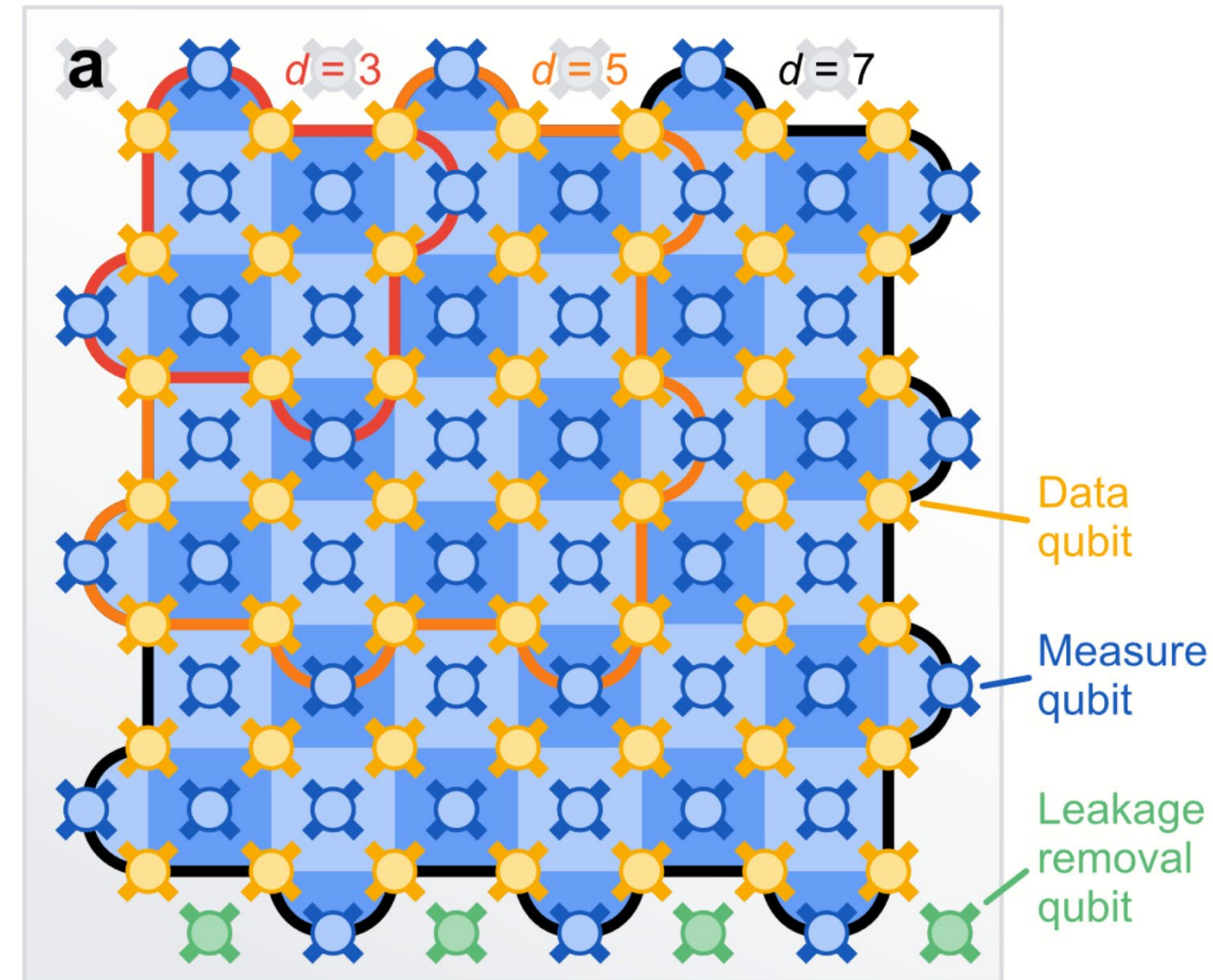
- Compare $\epsilon_L = 0.03$ to dominant physical error
 - Two-qubit gate error $\epsilon_{2Q} = 0.015$
 - Logical two-qubit gate error is expected to be dominated by ϵ_L
- Used simulations to project performance with physical error rates reduced by factor x
 - $\epsilon_L \propto 1/x^2$
 - Break-even within reach



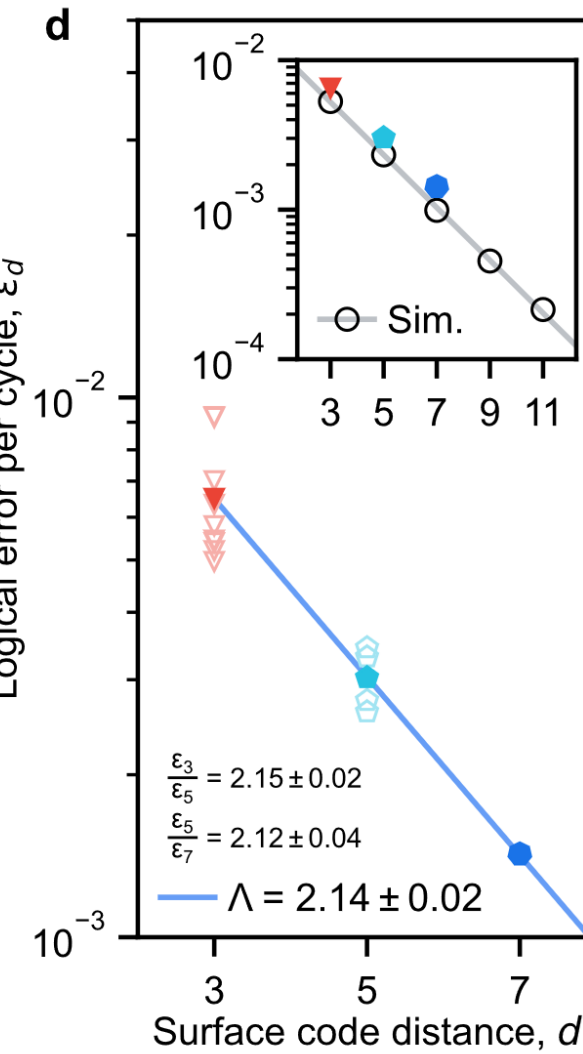
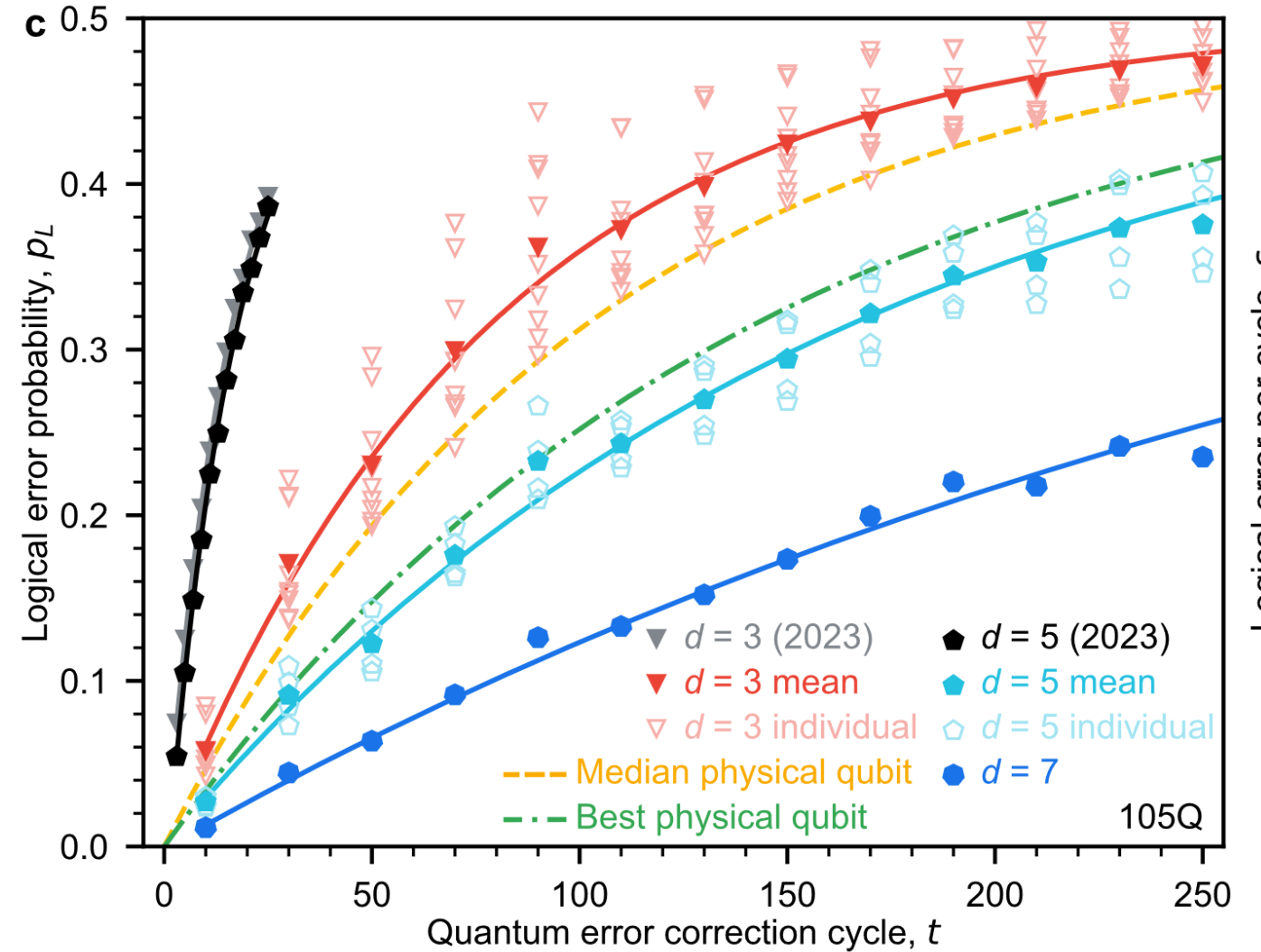
Error threshold

- $\epsilon_L \sim 0.03$ comparable to predicted logical error per cycle at error threshold
Fowler *et al.*, *Phys. Rev. A* **86**, 032324 (2012)
Stephens, *Phys. Rev. A* **89**, 022321 (2014).

Distance-Three, -Five and -Seven Surface Code Layout



Distance Scaling and Logical Error Suppression

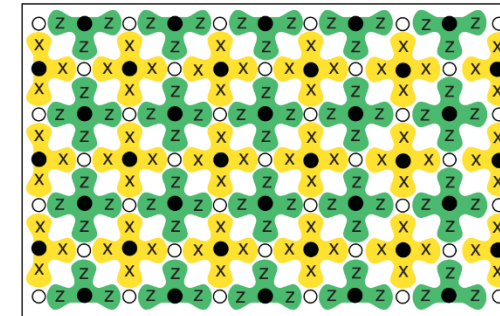


Surface Code and Lattice Surgery

- Surface code promising candidate for implementation of logical qubits in superconducting circuits

Kitaev, A. Ann. Phys. 303 1 (2003)

Fowler, A. et al. Phys. Rev. A 86, 032324 (2012)

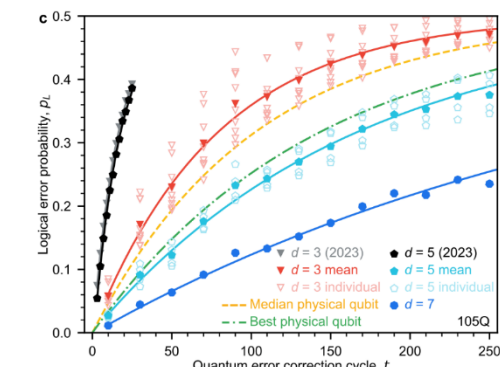


- Experimental realizations of logical state preservation near and beyond the threshold

Krinner, S. et al. Nature 605, pages 669–674 (2022)

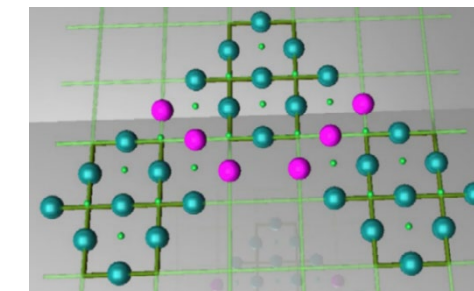
Google Quantum AI, Nature 614, pages 676–681 (2023)

Google Quantum AI and Collaborators, Nature (2024)



- Lattice surgery allows realization of non-transversal interactions between encoded qubits with low qubit-overhead

Horsman, D. et al. New J. Phys. 14 123011 (2012)



Experimental Work on Logical Qubit Operations

Logical operations on **encoded qubits**:

- Fault-tolerant subset of Clifford group on [4,2,2] code (s.c.)
[Harper, R. et al. Phys. Rev. Lett. 122, 080504 \(2019\)](#)
- Transversal CNOT on two [7,1,3] color codes (ions)
[Postler, L. et al. Nature 605, 675 \(2022\)](#)

Non-fault-tolerant **arbitrary state preparation**

- $d = 3$ Bacon-Shor code (ions)
[Egan, L. et al. Nature 598, 281 \(2021\)](#)
- $d = 3$ surface code (s.c.)
[Ye, Y. et al. Phys. Rev. Lett. 131, 210603 \(2023\)](#)

Lattice surgery ...

- ... on a $d = 2$ surface code (ions)
[Erhard, A. et al. Nature 589, 220 \(2021\)](#)
- ... on interleaved $d = 3$ 3CX and Bacon-Shor code (s.c.)
[Hetenyi, B. et al. PRX Quantum 5, 040334 \(2024\)](#)
- ... on a $d = 3$ color code (s.c.)
[Lacroix, N. et al., Nature \(2025\)](#)

Independent logical qubits during idling (modularity):

- transversal implementation of various QEC codes (ryd.)
[Bluvstein, D. et al. Nature 626, 58 \(2024\)](#)
- state teleportation on three $d = 3$ color codes (ions)
[Ryan-Anderson, C. et al. Science 385, 1327 \(2024\)](#)

Here: Modular lattice surgery on surface code with partial decoding
from repeated syndrome extraction on superconducting qubits

Transversal Gates vs. Lattice Surgery

All-to-all connectivity (ions, Rydberg atoms)

- Allows for transversal logical two-qubit gates

2D square lattice connectivity (s.c.)

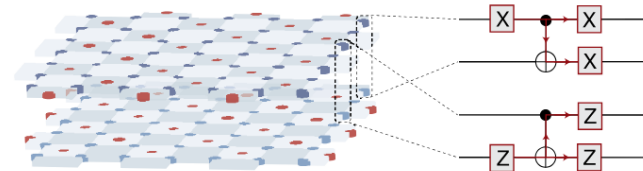
- Requires lattice surgery

Lattice surgery operations:

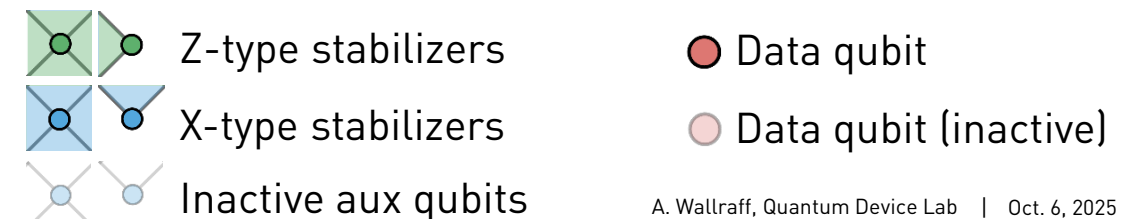
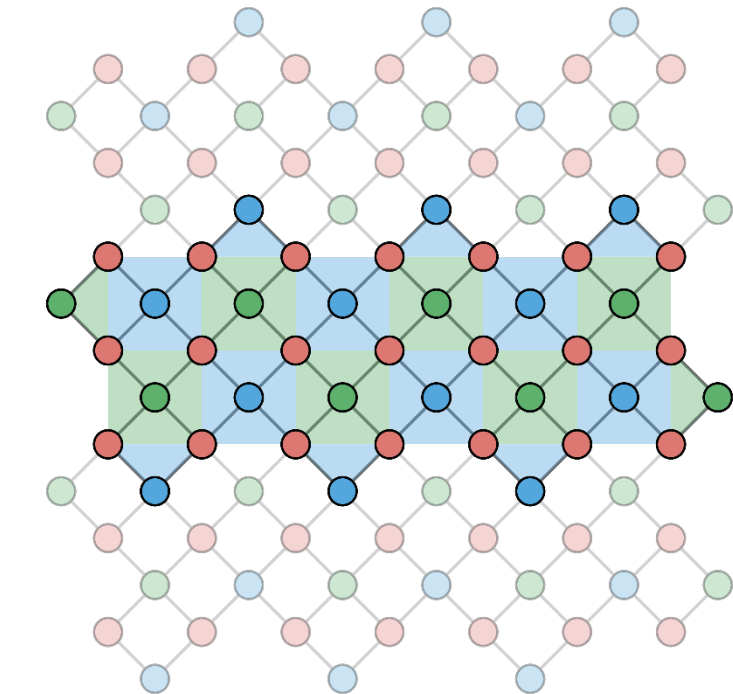
- Merge
- Split
- Measurement of logical two-qubit observables
 $\hat{X}_{L1}\hat{X}_{L2}$ (or $\hat{Z}_{L1}\hat{Z}_{L2}$)

Horsman, D. et al. New J. Phys. 14 123011 (2012)

Austin G. Fowler, Craig Gidney arXiv:1808.06709 (2018)

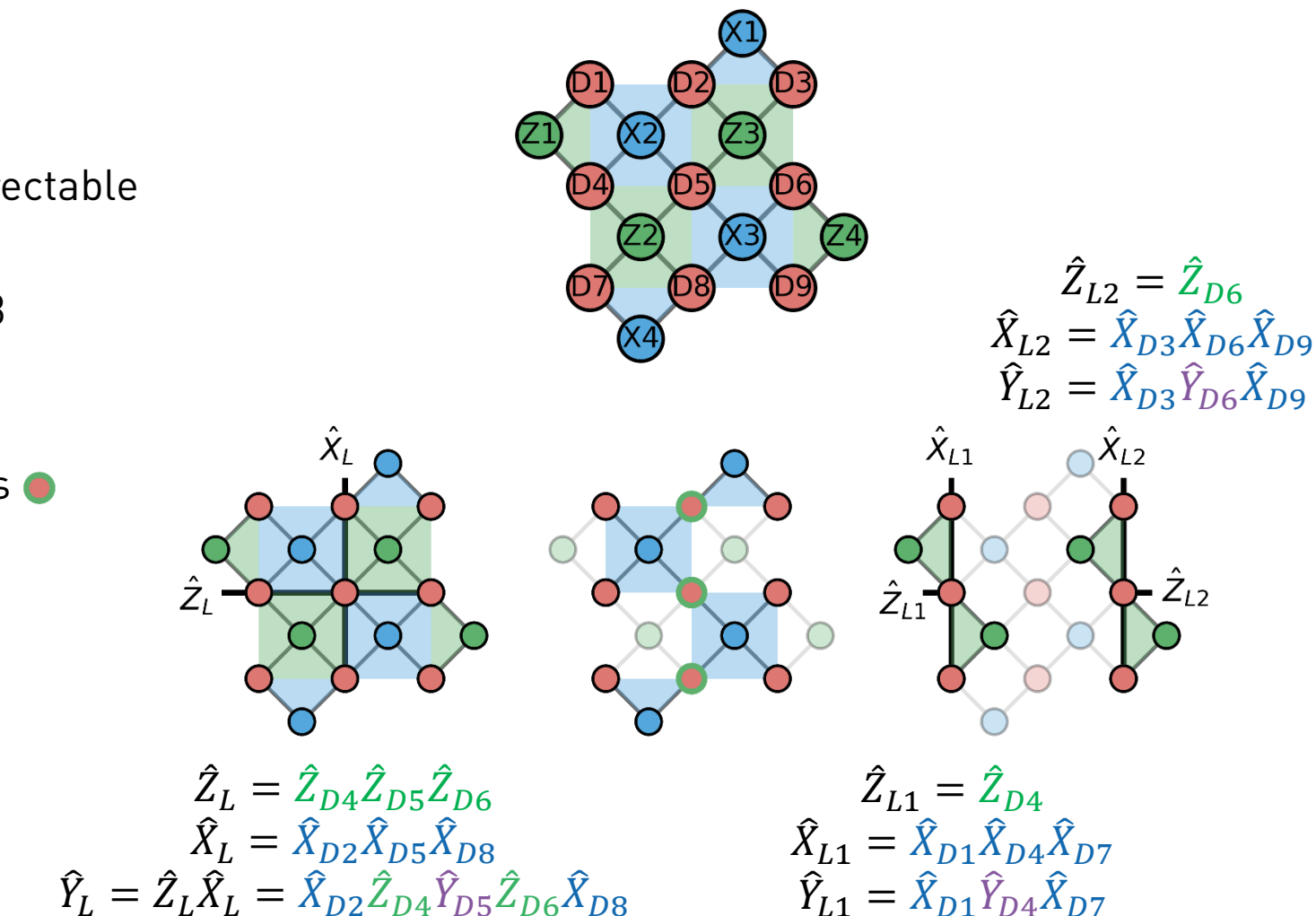


D. Bluvstein et al, Nature 626, pages 58–65 (2024)



Logical Operators of the Surface and the Repetition Codes

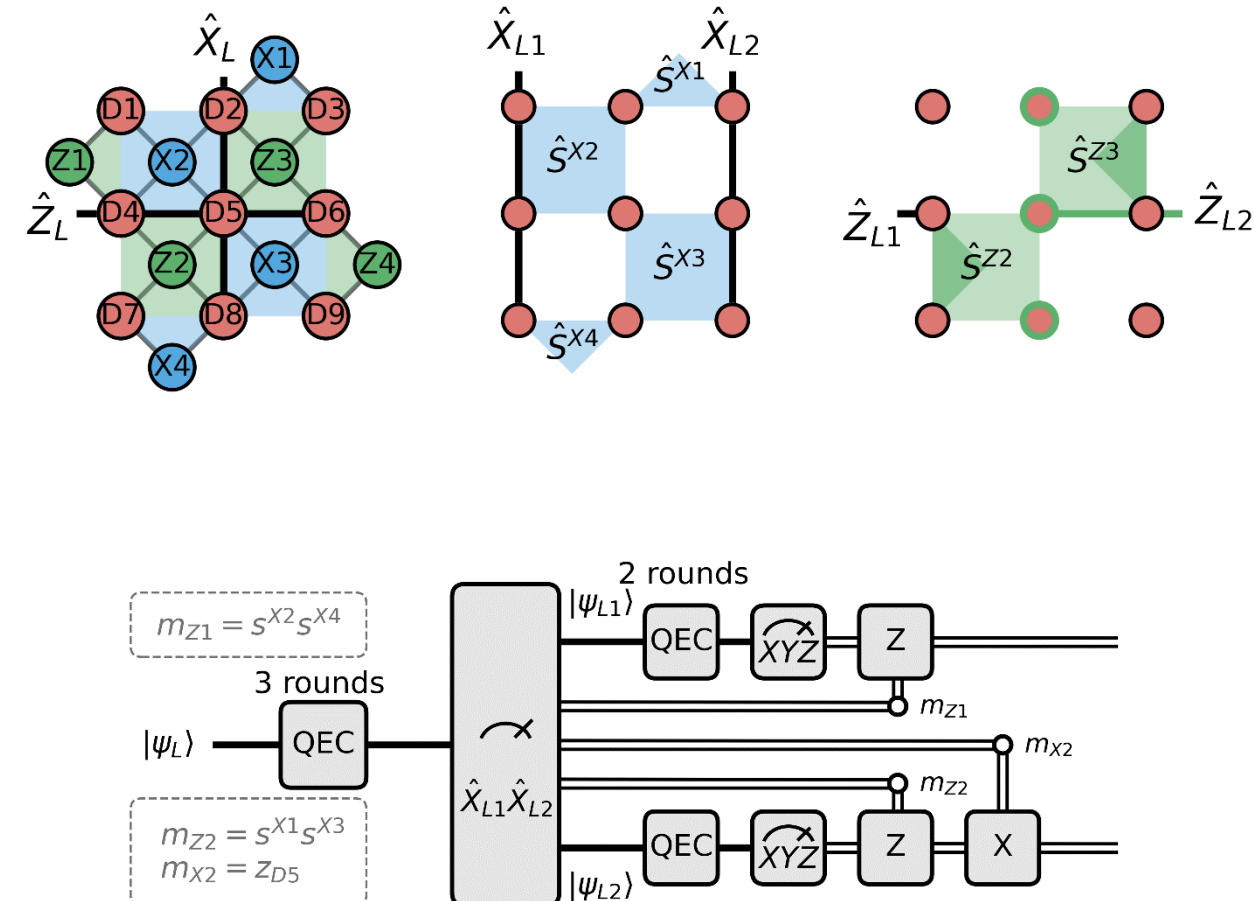
- Distance-three surface code qubit:
 - 3×3 patch on the data qubit lattice,
 - single bit-flip and phase-flip errors correctable
 - Logical operator definitions
- Lattice split operation transforms the $d = 3$ surface code into two $d = 3$ bit-flip codes:
 - Stop measuring X-type stabilizers
 - Readout of middle column of data qubits in Z-basis
- Two $d = 3$ bit-flip repetition codes:
 - Two 1×3 patches
 - Single bit-flip error correctable
 - Logical operator definitions



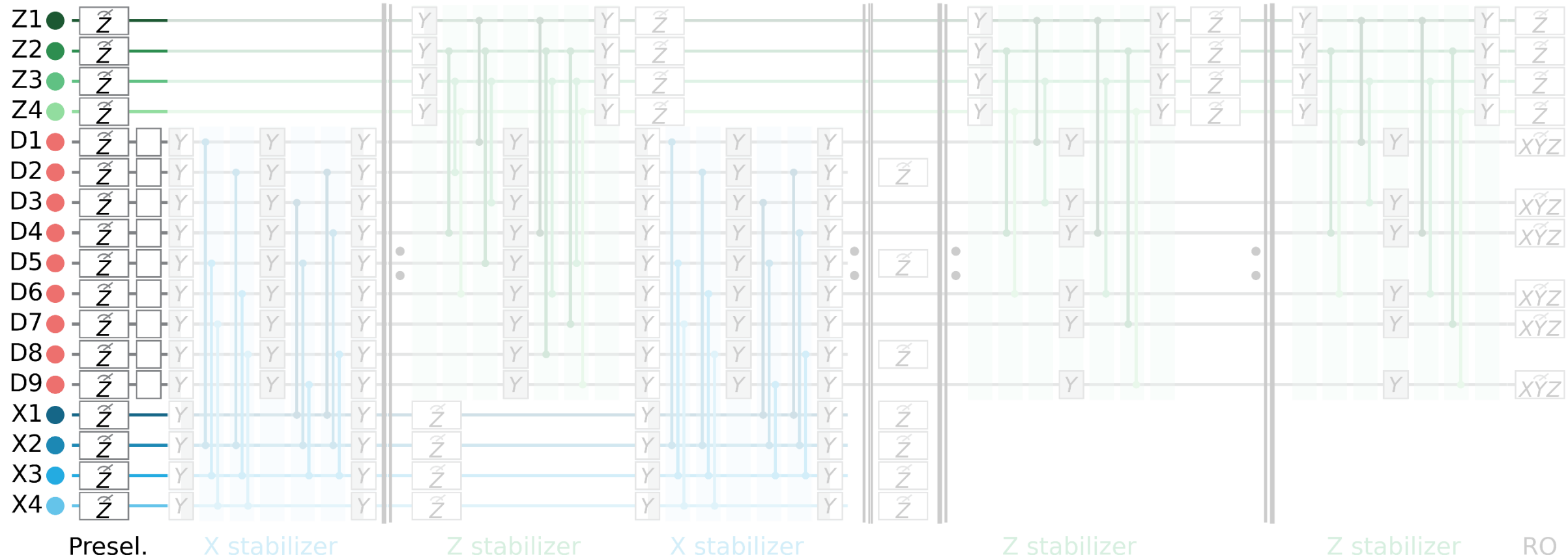
Pauli Frame Update

- Logical states after split depend on measurement outcomes
- Relation between repetition and surface code logical operators
 - Logical X-operators:
$$\hat{X}_{L1} = \hat{X}_L \hat{S}^{X2} \hat{S}^{X4}$$

$$\hat{X}_{L2} = \hat{X}_L \hat{S}^{X1} \hat{S}^{X3}$$
- Logical Z-operators:
$$\hat{Z}_L = \hat{Z}_{D4} \hat{Z}_{D5} \hat{Z}_{D6} = \hat{Z}_{L1} (\hat{Z}_{L2} \hat{Z}_{D5})$$
- Deterministic operation realized by feed-forward Pauli-Frame update:
 - $\hat{X}_L \rightarrow \hat{X}_{L1}, \hat{X}_{L2}$
 - $\hat{Z}_L \rightarrow \hat{Z}_{L1} \hat{Z}_{L2}$
 - performed in post-processing
- Weight-4 Z-type stabilizers become weight-2, value updated by data qubit readout outcome



Gate Sequence of Lattice-Split Operation

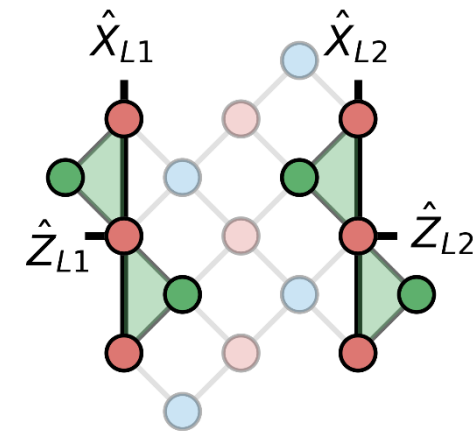


Y Y Y Single-qubit Y rotation $(-\frac{\pi}{2}, \pi, \frac{\pi}{2})$
I CZ gate

- **Qubit initialization**
- **X-syndrome extraction to initialize d = 3 qubit**
- **Three rounds of syndrome extraction**
- **Lattice split**
- **Two rounds of syndrome extraction**
- **Logical observable readout**

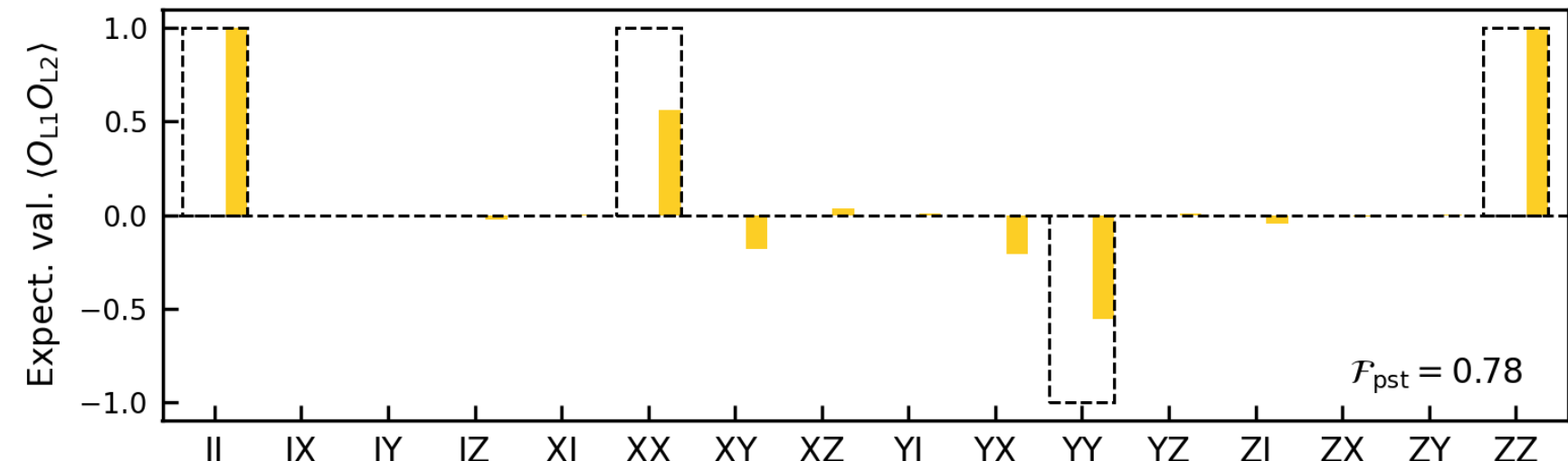
Logical Bell State Creation

- Prepare surface-code $|0\rangle_L$ and perform lattice split
- Fault-tolerant ($d = 3$) with respect to **bit-flip errors**
- Non-fault-tolerant ($d = 1$) with respect to **phase-flip errors**
- Evaluate Logical Bell state after **Pauli-frame update**:
 - Ideally $X_{L1}X_{L2} = Z_{L1}Z_{L2} = 1$ and $Y_{L1}Y_{L2} = -1$
- ~70'000 shots per logical operator, reject leakage, and calculate **expectation values**



Logical State Tomography

- Measure **all nine basis combinations of repetition code logical qubits** to perform **logical quantum state tomography**
- Use extracted syndromes to **post-select** on zero syndrome elements (no error)
 - $Z_{L1}Z_{L2}$ error <1%: **fault tolerant** with respect to **bit-flips**
 - Expectation value of $X_{L1}X_{L2}$ and $Y_{L1}Y_{L2}$ limited by repetition code

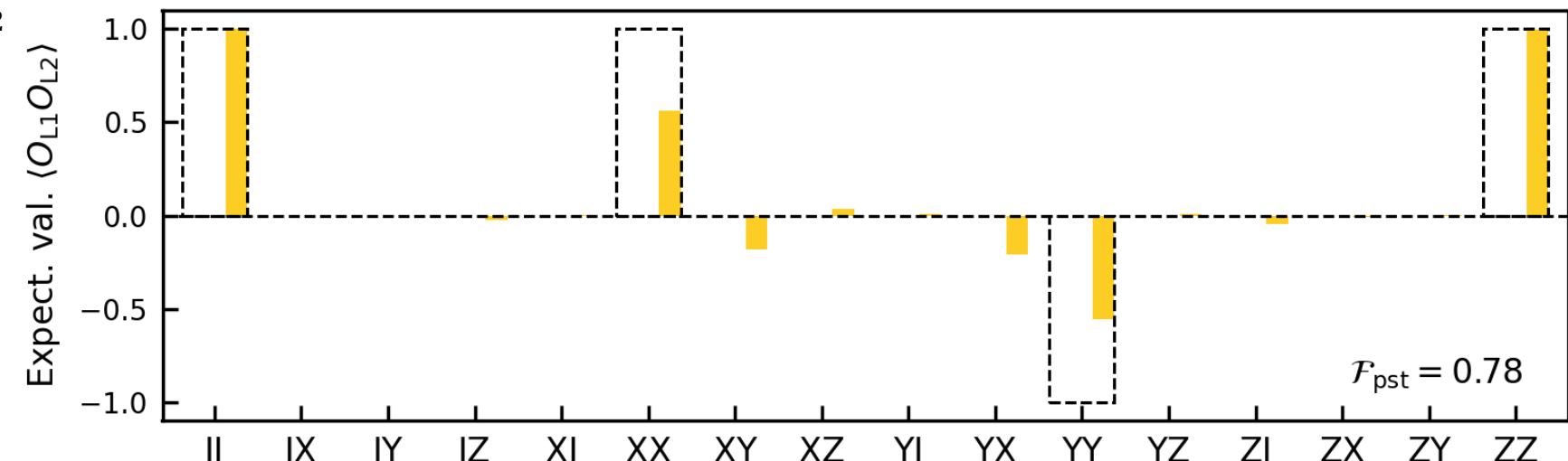


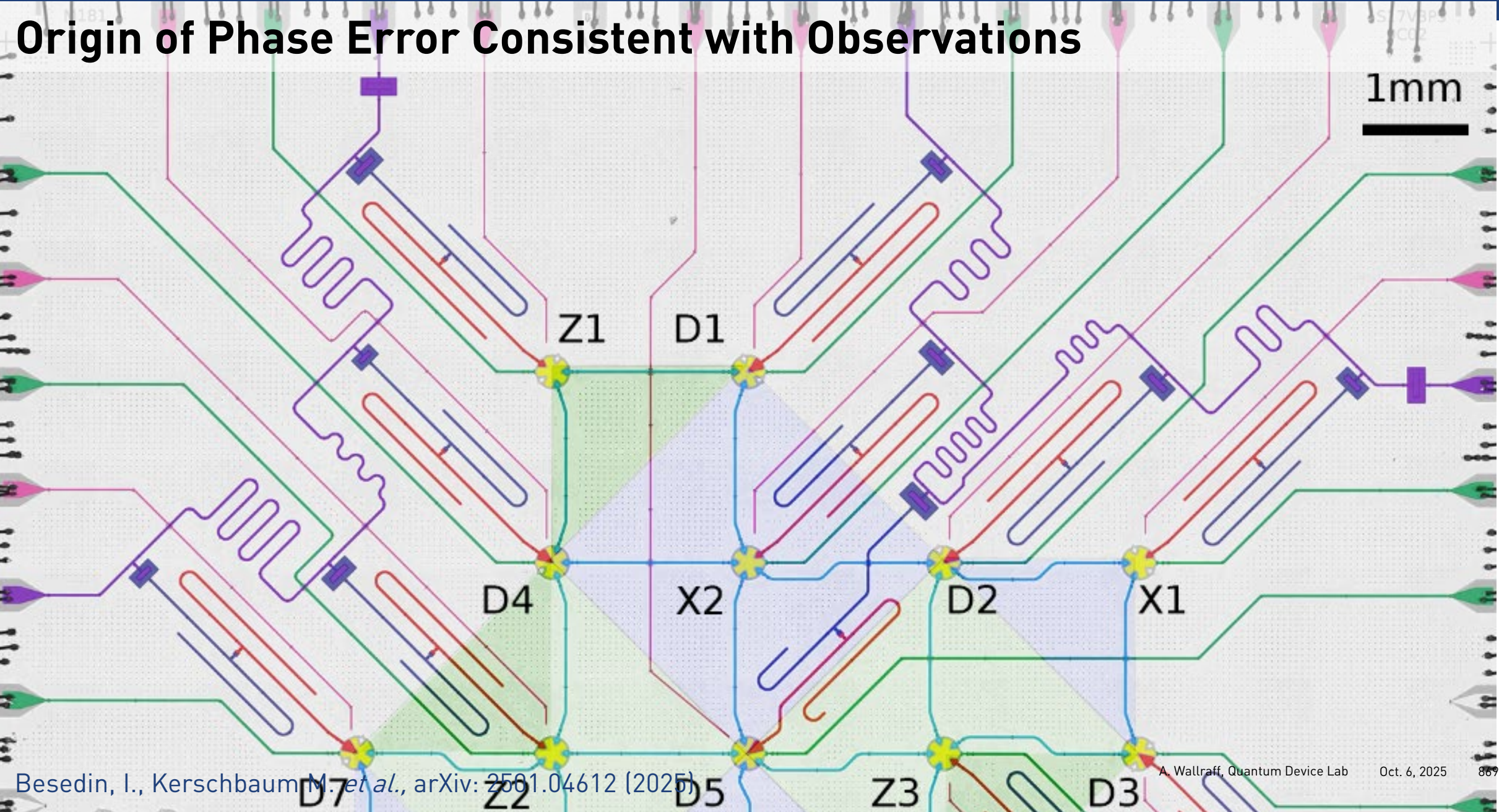
Logical State Tomography

- Measure **all nine basis combinations of repetition code logical qubits** to perform **logical quantum state tomography**

Note

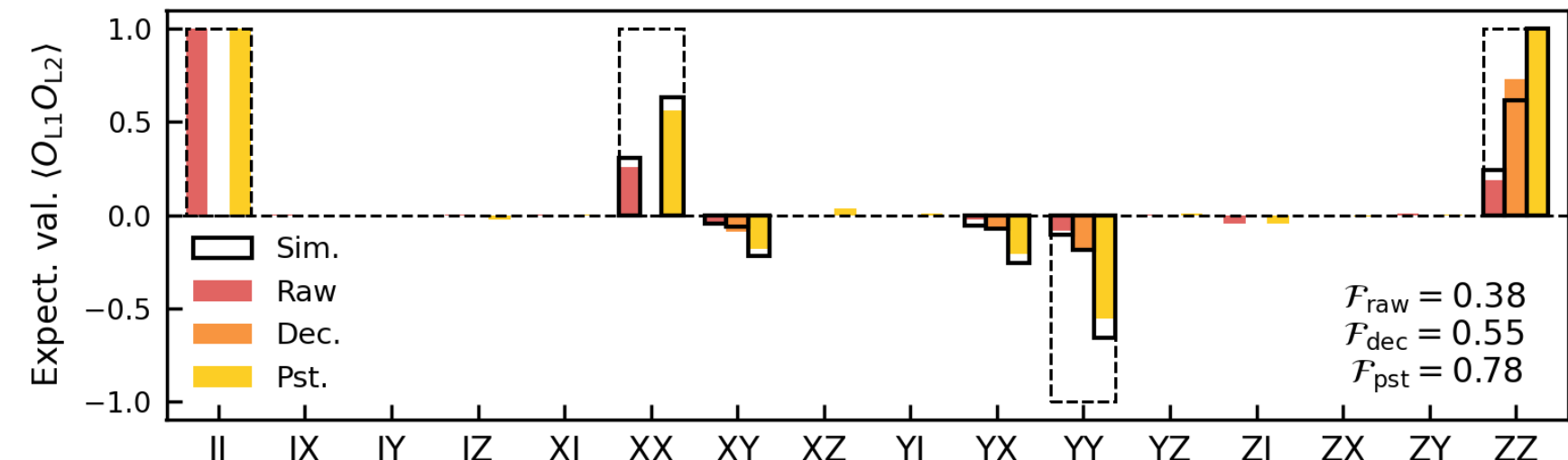
- Non-zero $X_{L1}Y_{L2}$ and $Y_{L1}X_{L2}$ expectation values
- Consistent with a 0.11π phase error on the first logical qubit state





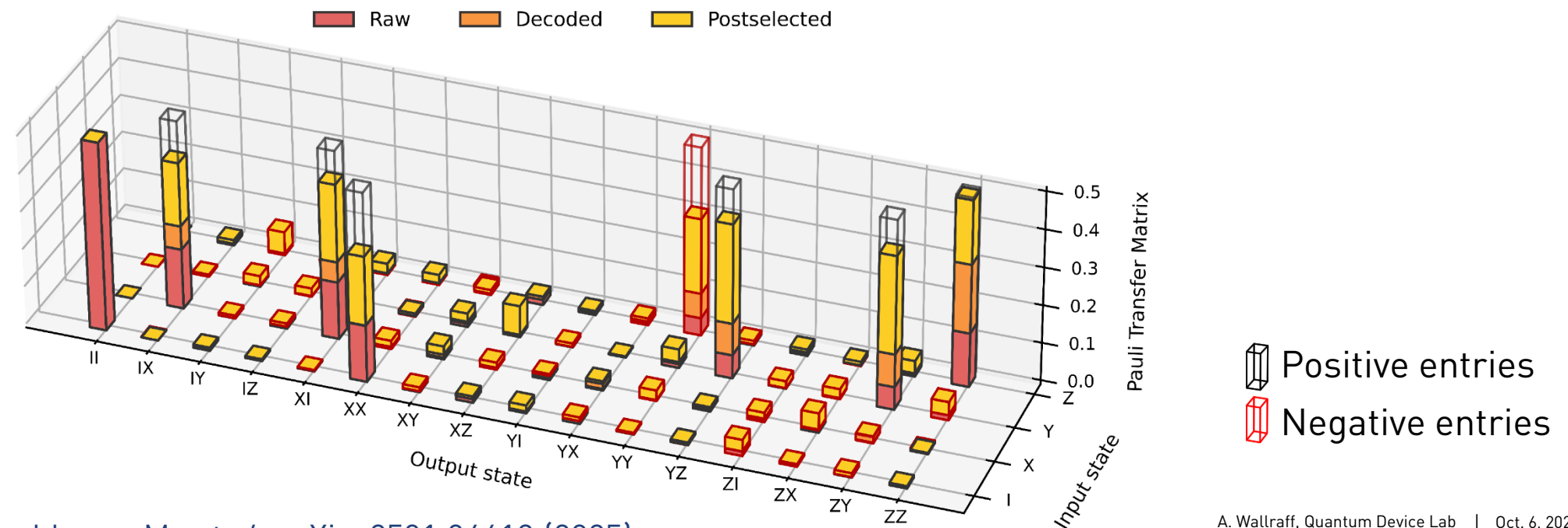
Logical State Tomography

- Measure **in all nine combinations of bases of logical qubits** to perform **logical quantum state tomography**
- Use **MWPM decoder**:
 - raw $Z_{L1} Z_{L2} = 0.19$ is improved to 0.73
- Good agreement of data with Pauli error model **simulations** based on randomized benchmarking (RB) and coherence measurements (+ coherent error on D1)



Logical Quantum Process Tomography

- Split acting on logical input states $|0\rangle_L, |1\rangle_L, |+\rangle_L, |-\rangle_L, |+i\rangle_L, |-i\rangle_L$ states
- Split operation maps Pauli operators to Pauli operators
- Note: single-qubit phase rotation of 0.11π on logical qubit 1 corrected for.
- Pauli transfer matrix (PTM) representation
 - ideal values $\pm 1/2$
- Process fidelity
 - raw: $\mathcal{F} = 0.310(12)$
 - decoded: $\mathcal{F} = 0.442(12)$
 - post-selected: $\mathcal{F} = 0.80(3)$

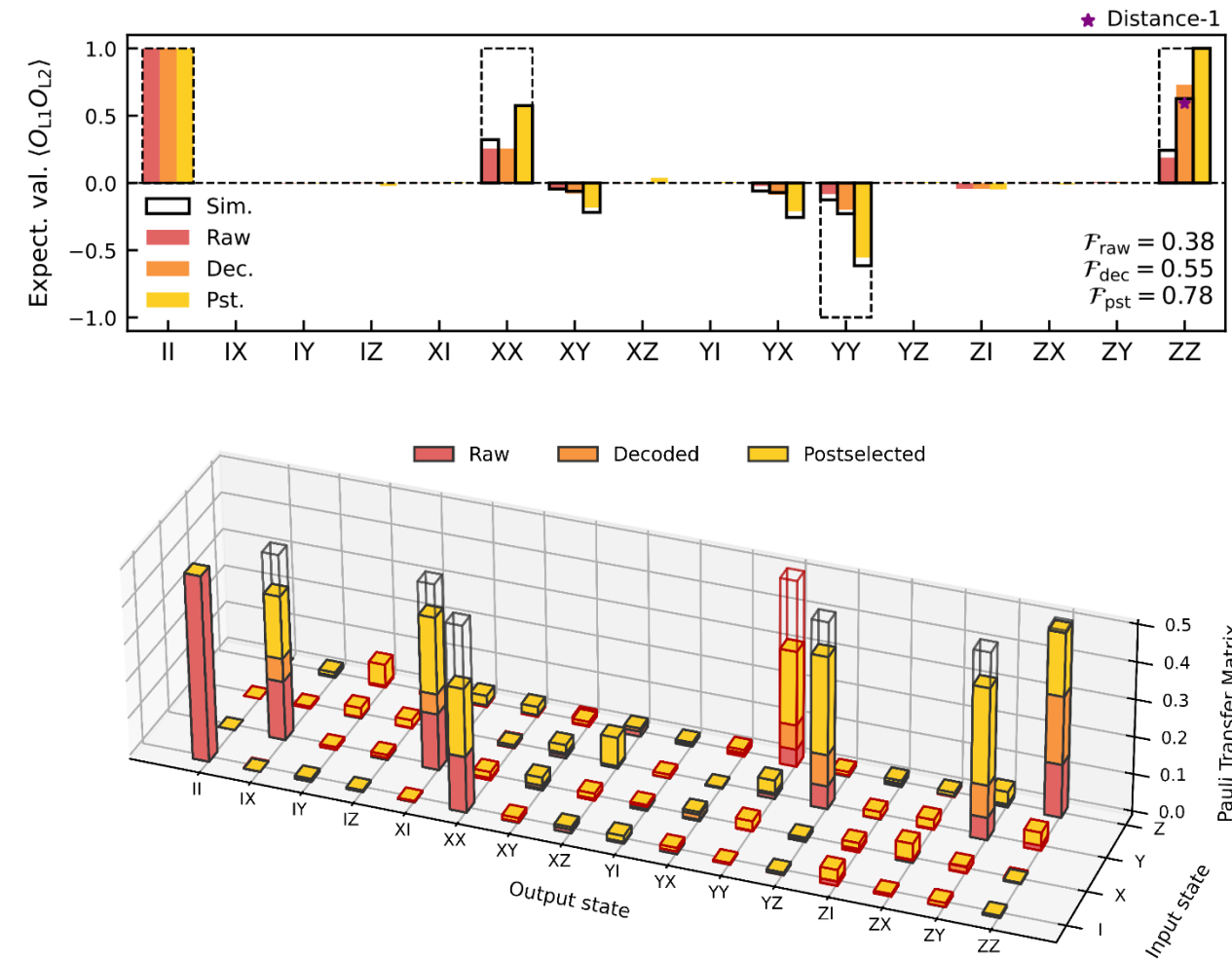


Summary and Outlook

- Demonstrated **lattice surgery** on a distance-three surface code, **creating a logical Bell state** of two distance-three repetition codes
- Increased decoded observable expectation value** compared to non-encoded variant
- Measured **logical Pauli-transfer matrix** for lattice split operation

Outlook

- Deploy full scheme on two distance-three surface codes and integrate in **logical state teleportation protocol**



The Quantum Device Lab



**Schweizerischer
Nationalfonds**

Innovation project
supported by



Schweizerische Eidgenossenschaft
Confédération suisse
Confederazione Svizzera
Confederaziun svizra
Swiss Confederation
Innosuisse – Swiss Innovation Agency



IARPA
BE THE FUTURE

with spring-term project students

**Want to work with us?
Looking for Grad Students, PostDocs and Technical Staff.**

